European Journal of Agronomy 174 (2026) 127977

Contents lists available at ScienceDirect

European Journal of Agronomy

journal homepage: www.elsevier.com/locate/eja

Development and validation of a crop yield prediction framework accounting for regional heterogeneity: A case study of spring maize in Jilin Province

Jun Gao [a], Daming Dong [b,c,*], Wenjiang Huang [d,e,f], Yingying Dong [d,e,f], Tongren Xu [g], Chongya Jiang [h,i,j,k], Kun Wang [d,e,f,**]

[a] School of Information and Artificial Intelligence, Anhui Agricultural University, Hefei 230036, China
[b] Key Laboratory of Agricultural Sensors, Ministry of Agriculture and Rural Affairs, Beijing Academy of Agriculture and Forestry Sciences, Beijing 100097, China
[c] National Research Center of Intelligent Equipment for Agriculture, Beijing Academy of Agriculture and Forestry Sciences, Beijing 100097, China
[d] State Key Laboratory of Remote Sensing and Digital Earth, Aerospace Information Research Institute, Chinese Academy of Sciences, China
[e] Sino-UK Pest and Disease Forecasting & Management Joint Laboratory, China
[f] University of Chinese Academy of Sciences, Beijing 100049, China
[g] State Key Laboratory of Earth Surface Processes and Disaster Risk Reduction, Faculty of Geographical Science, Beijing Normal University, Beijing 100875, China
[h] National Engineering Technology Center for Information Agriculture, Nanjing 210095, China
[i] Intelligent Agriculture Engineering Research Center, Ministry of Education, Nanjing 210095, China
[j] Key Laboratory for Crop System Analysis and Decision Making, Ministry of Agriculture and Rural Affairs, Nanjing 210095, China
[k] Jiangsu Key Laboratory for Information Agriculture, Nanjing 210095, China

ARTICLE INFO

Keywords:
Crop model
Data assimilation
Deep learning
Yield prediction
Early forecasting

ABSTRACT

Accurate and timely crop-yield prediction is essential for ensuring food security, managing agricultural risk, and supporting policy formulation. To address the respective limitations of traditional crop growth models and deep learning methods under complex environmental conditions, a hybrid modeling framework is proposed that integrates remote-sensing data assimilation, a process-based crop growth model, and deep learning techniques. Using spring maize in Jilin Province, China (2015–2020) as the case study, leaf area index (LAI) retrieval accuracy is first improved by coupling the PROSAIL model with machine-learning algorithms. A complete meteorological sequence for the target year is then constructed using a dynamic time warping (DTW) algorithm to overcome early-season prediction challenges caused by missing real-time weather data. Retrieved LAI is assimilated into the WOFOST crop growth model through an ensemble Kalman filter (ENKF) to calibrate state variables and enable dynamic yield prediction across growth stages. Finally, a deep learning model (Convolutional Neural Network–Attention Long Short-Term Memory with Multi-Task Learning, CNN-ALSTM-MTL) is developed to fuse assimilation outputs with multi-source heterogeneous data, leveraging multi-task learning to enhance adaptability to regional heterogeneity and improve yield prediction performance at the regional scale. Assimilation is found to substantially improve maize-yield estimation, increasing R^2 by 0.2 and reducing RMSE by 276 kg ha^{-1}. Compared with the assimilated crop growth model alone, the hybrid framework further increases R^2 by 35 % and decreases RMSE by 23 % by hierarchically capturing feature information relevant to maize-yield estimation. The best performance is achieved during the key growth stage (jointing to tasseling stage), with an R^2 of 0.75 and an RMSE of 592 kg ha^{-1}, enabling reliable yield prediction approximately two months before harvest. This framework demonstrates potential for cross-crop and cross-regional applications and provides robust methodological support for regional-scale yield forecasting and food-security early warning.

* Corresponding author at: Key Laboratory of Agricultural Sensors, Ministry of Agriculture and Rural Affairs, Beijing Academy of Agriculture and Forestry Sciences, Beijing 100097, China.
** Corresponding author at: State Key Laboratory of Remote Sensing and Digital Earth, Aerospace Information Research Institute, Chinese Academy of Sciences, China.
E-mail addresses: dongdm@nercita.org.cn (D. Dong), wangk@aircas.ac.cn (K. Wang).

https://doi.org/10.1016/j.eja.2025.127977
Received 27 August 2025; Received in revised form 19 December 2025; Accepted 29 December 2025
Available online 2 January 2026
1161-0301/© 2025 Elsevier B.V. All rights are reserved, including those for text and data mining, AI training, and similar technologies.

1. Introduction

With the continued growth of the global population and rising living standards, food demand is expected to increase substantially by the mid-twenty-first century. The Food and Agriculture Organization of the United Nations (FAO) projects that global food demand will rise by approximately 70 % by 2050 relative to current levels (Falcon et al., 2022). As one of the world's most important staple crops, maize is of particular concern due to its rapidly increasing demand. Under the uneven spatial distribution of climate resources and cultivation conditions, food security depends not only on overall production increases but also on the ability to generate timely forecasts for specific regions and growing seasons. Therefore, reliable in-season yield prediction is essential for supporting governmental regulatory decisions and for enabling local optimization of planting strategies and input management (Basso and Liu, 2019; Brown et al., 2018).

Crop-yield prediction methods can be broadly classified into three categories: process-based crop growth models, statistical regression models, and emerging artificial-intelligence models. Process-based models simulate crop growth and development, effectively capturing interactions between crops and their environment and providing an important tool for understanding crop growth mechanisms (Wanthanaporn et al., 2024; Chen et al., 2020). However, these models often require numerous input parameters, involve substantial uncertainty, and show limited applicability when meteorological conditions deviate markedly from normal patterns (Moriondo et al., 2011; Semenov and Porter, 1995). Statistical regression models establish relationships between meteorological factors and yield based on historical data and are relatively simple to operate, but they struggle to accurately represent complex nonlinear relationships (Lobell and Burke, 2010; Ansarifar et al., 2021; Conradt, 2022). In recent years, machine-learning and deep-learning models have shown substantial potential in yield prediction owing to their strong nonlinear fitting capability. For example, some studies explore two directions—time-series and multimodal modeling, and lightweight model fusion: Lu et al. (2025a, 2025b) integrate hyperspectral data with a QRBiLSTM-MHSA architecture to perform interval prediction of rice yield (Lu et al., 2025a, 2025b); IMobileTransformer combines MobileNet with an improved Transformer to balance accuracy and efficiency in rice disease identification (Lu et al., 2025a, 2025b). Despite these advances in accuracy and efficiency, model interpretability still requires further improvement.

To reduce uncertainty in crop growth models, data assimilation techniques can be employed to dynamically integrate multi-source data from satellite remote sensing, ground observations, and other sources with model prediction results.This integration enables real-time optimization of model states and parameters, substantially enhancing predictive accuracy and offering new avenues for model improvement (De Wit and Van Diepen, 2007; Zare et al., 2024; Luo et al., 2023; Ines et al., 2013). Data assimilation proves particularly advantageous for in-season yield forecasting, where timely updates are critical. Nevertheless, even with assimilation, crop models continue to face challenges in capturing crop responses to extreme climate events. These limitations arise primarily from the oversimplification of key physiological processes within the models (Chen and Tao, 2022).

To address these issues, previous research has proposed hybrid approaches that couple crop models with machine-learning techniques. For example, combining APSIM with random forest algorithms for winter wheat in the North China Plain improves yield prediction under extreme climate conditions (Bai et al., 2024). Such hybrid methods retain the mechanistic representation of physiological processes in crop models while leveraging the strong nonlinear fitting ability of machine learning to enhance predictive performance. This integration helps compensate for the limitations of individual models and offers more accurate and reliable solutions for crop-yield prediction, particularly in evaluating the impacts of extreme climate events (Sajid et al., 2022; Alimagham et al., 2025; Feng et al., 2020; Li et al., 2023a, 2023b; Hu et al., 2024). Although current studies have demonstrated the advantages of combining crop growth models with machine learning, existing work primarily focuses on reducing prediction deviations caused by anomalous meteorological conditions. Spatial heterogeneity within regions has rarely been considered, and simply coupling "crop growth models + machine learning" does not automatically distinguish such spatial structures. As a result, county-level predictive accuracy may still fluctuate across different subregions. Therefore, to further improve yield-prediction performance, it is necessary to systematically integrate crop growth models, multi-source data assimilation, and artificial intelligence into a unified framework tailored to spatially heterogeneous environments. Such multi-technology collaboration offers a promising pathway for enhancing the accuracy and robustness of crop-yield prediction (Zhuang et al., 2024).

This study proposes an innovative multi-level hybrid modeling framework that integrates remote-sensing data assimilation, a process-based crop growth model, and deep learning techniques to improve the accuracy and timeliness of maize yield prediction. County-level yield prediction is evaluated for typical climatic years in the context of regional heterogeneity. First, the framework couples a radiative-transfer model with a crop growth model, and model performance is enhanced through parameter calibration and data assimilation. Building on this foundation, deep learning is incorporated to leverage its strengths in feature extraction and nonlinear representation, further increasing predictive performance. Within this methodological framework, the study addresses three key questions: 1) Under meteorological sequences generated by the dynamic time warping (DTW) algorithm, how does assimilating retrieved leaf area index (LAI) into the WOFOST model influence prediction performance across different growth stages? 2) To what extent does the hybrid framework, which combines the assimilated crop model with deep learning, improve performance under regional heterogeneity? 3) How robust and adaptable is this framework in different regional environments, and which growth stage corresponds to its optimal prediction window?

2. Materials and methods

2.1. Study area

The study area is located in Jilin Province in Northeast China, spanning 40°52′–46°18′N and 121°38′–131°19′E. The eastern region is dominated by the Changbai Mountains, the central part consists of the Songnen Plain, and the western part transitions into the Horqin Grassland, forming a pronounced topographic pattern that is "higher in the east and lower in the west." Elevation gradually decreases from 2691 m in the east to approximately 140 m in the western plain. The region is characterized by a temperate continental monsoon climate with strong seasonality. The mean annual temperature ranges from 2 °C to 6 °C, and annual precipitation increases from about 400 mm in the west to 900 mm in the east, with 70 % of the rainfall occurring between June and August. From the perspective of thermal resources, a stable east–west gradient of growing degree days (GDD) is observed across the province, with isotherms decreasing progressively from west to east.

As one of China's major commercial grain-producing regions, Jilin Province allocates nearly 60 % of its arable land to spring maize cultivation. Due to its distinct geographical and climatic conditions, spring maize is typically sown from late April to early May and harvested in late September, with a growing period of approximately 130 days. To ensure spatial representativeness, seven agro-meteorological stations are selected from across Jilin's principal agricultural zones (Fig. 1). These stations encompass a range of topographic, climatic, and soil conditions, providing a comprehensive characterization of the agro-climatic environment in Jilin's spring maize-growing regions.

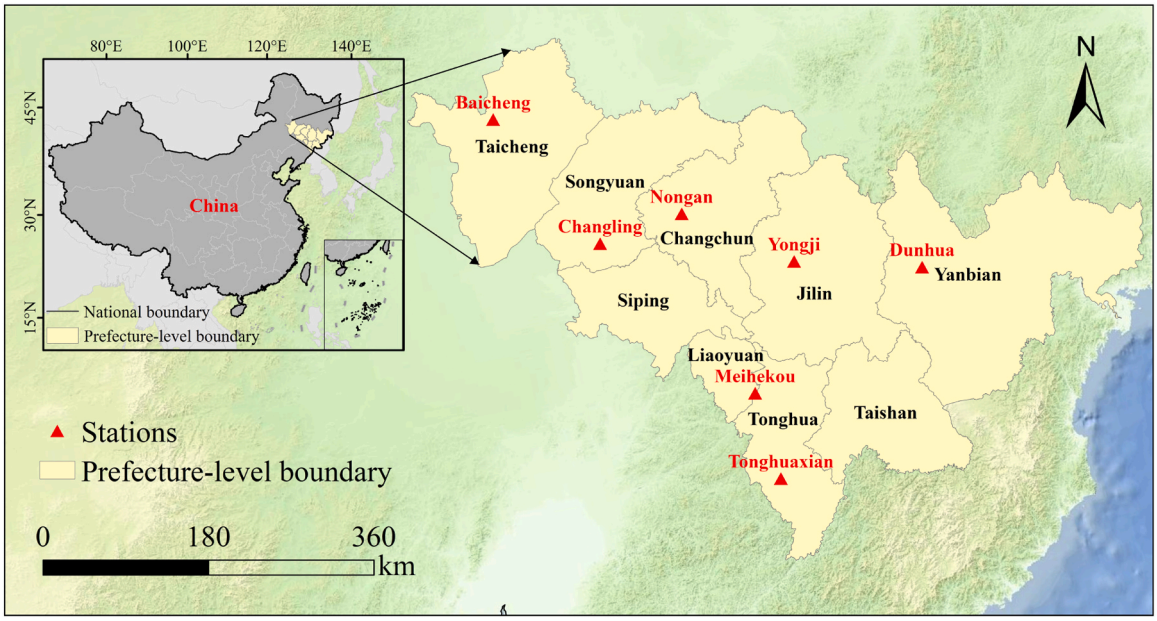


Fig. 1. Distribution of agrometeorological stations for spring maize in Jilin Province.

2.2. Data types and acquisition methods

2.2.1. Landsat 8 imagery

Remote sensing reflectance data are obtained from the Operational Land Imager (OLI) sensor onboard the Landsat-8 satellite, which has been in operation since 2013. The sensor provides a spatial resolution of 30 m and a revisit interval of 16 days. Surface reflectance data used in this study are sourced from the Landsat 8 Collection 2, Tier 1 Level-2 product (Landsat/LC08/C02/T1_L2) available on the Google Earth Engine platform. The selected spectral bands include blue (B2, 0.45–0.51 μm), green (B3, 0.53–0.59 μm), red (B4, 0.63–0.67 μm), near-infrared (B5, 0.85–0.87 μm), and two shortwave infrared bands (B6 and B7). All bands have undergone radiometric calibration and atmospheric correction, ensuring the data quality is suitable for high-precision agricultural monitoring applications.

2.2.2. MODIS LAI imagery

Leaf Area Index (LAI) data are obtained from the MODIS LAI product (MODIS/061/MOD15A2H), which is provided by NASA with a spatial resolution of 500 m and a temporal resolution of 8 days. LAI represents the ratio of total leaf surface area to the ground area, serving as a critical parameter in studies of ecosystem productivity, climate, and hydrology. As a Level-4 MODIS product, it offers a continuous time series of global LAI data since 2000 and has been widely used for monitoring and analyzing vegetation dynamics. In this study, the MODIS LAI product is used to validate the LAI retrieval results derived from a radiative transfer model coupled with machine learning algorithms.

2.2.3. NDVI data

The MOD13Q1 V6.1 product (MODIS/061/MOD13Q1) provides gridded vegetation index data at a 16-day temporal resolution and 250-meter spatial resolution. This dataset captures vegetation growth dynamics and reflects photosynthetic activity throughout the maize growing season. By applying atmospheric correction algorithms and cloud-masking techniques, the product effectively mitigates interference from aerosols and cloud cover, thereby improving both temporal continuity and spatial consistency of vegetation indices. Due to its high temporal and spatial resolution, MOD13Q1 demonstrates strong performance in crop growth monitoring. It enables accurate tracking of maize development during key phenological stages and offers a reliable basis for quantifying the crop growth processes that determine yield formation.

2.2.4. Meteorological data

Meteorological data are primarily obtained from 7 agro-meteorological observation stations located within the study area, provided by the China Meteorological Administration through its National Meteorological Data Service Center (http://data.cma.cn). The dataset includes daily maximum temperature, minimum temperature, vapor pressure, wind speed, and precipitation. Given the limited spatial coverage of these ground-based stations, supplementary meteorological data are sourced from the ERA5-Land reanalysis product available on the Google Earth Engine (GEE) platform to fill gaps in areas not directly covered by in-situ observations.

2.2.5. Soil data

Soil data are obtained from the China soil dataset within the Harmonized World Soil Database (HWSD). This dataset provides essential input parameters for crop modeling, including clay, sand, gravel, silt content, organic matter, and bulk density. These variables characterize the physical environment and resource base necessary for crop growth.

2.2.6. Phenological data

Key phenological stages of maize were identified by integrating interpolated planting dates from seven agro-meteorological stations (2015–2020) with a maize phenology dataset from the China National Ecological Science Data Center (https://www.escience.org.cn/), covering the period from 2001 to 2020. This dataset, developed by the Global Change and Terrestrial Ecosystem Modeling Research Team at Peking University, is derived from a long-term, high spatiotemporal resolution fused NDVI dataset and annually updated maize distribution maps. Phenological stages are determined using a relative threshold method. Based on this information, the maize growing season is divided into four developmental stages: T1: sowing to three-leaf stage, T2: three-leaf to jointing stage, T3: jointing to tasseling stage, and T4: tasseling to maturity stage.

2.2.7. Maize planting area

Maize distribution data for the study area during 2015–2020 are

obtained from the China Maize Planting Distribution Dataset (2001–2024), provided by the Global Change and Terrestrial Ecosystem Modeling Research Team at Peking University (Fig. 2). This dataset is generated using the Time-Weighted Dynamic Time Warping (TWDTW) algorithm, based on a high spatiotemporal resolution fused remote sensing dataset.

2.2.8. Yield data

County-level maize yield data for Jilin Province from 2015 to 2020 are obtained from the National Bureau of Statistics of China. The dataset covers the primary maize-producing regions, with all prefecture-level districts and county-level cities uniformly categorized as county-level units.

2.3. Data preprocessing

2.3.1. Variable construction and processing

This study integrates multi-source data to enhance the accuracy of maize yield estimation. The model uses county-level maize yield as the output variable, with input features derived from remote sensing, meteorological observations, soil data, and crop model simulations incorporating data assimilation. The sources and purposes of the original datasets are summarized in Table 1. Several derived input variables—including growing degree days (GDD), heat degree days (KDD), frost degree days (FDD), and extreme precipitation index (EPA)—are calculated from raw meteorological data (Tmax, Tmin, and PRCP), with detailed formulas provided in Supplementary Text S1. All other input features are directly extracted from the original datasets without further transformation.

To ensure spatial consistency across datasets, all variables are masked based on the 2015–2020 maize planting distribution (Fig. 2) at the county level and uniformly resampled to a spatial resolution of 1 km. The retained maize pixels within each county are then averaged and aggregated to generate county-level features for subsequent modeling.

Table 1
Data collection and sources.

Data Type	Variable	Descriptions	Usage	Sources
Maize phenology data	/	/	Define maize growing season	China National Ecological Science Data Center
Maize planting distribution	/	/	Define maize planting distribution	China National Ecological Science Data Center
Maize yield data	Yield	Maize yield per unit area	Model output labels	Agricultural Statistics Yearbook
Remote sensing data	NDVI	Normalized Difference Vegetation Index	Model inputs	MOD13Q1 V6.1
Meteorological data	Tmax, Tmin, Wind, Vap, PRCP	Highest temperature, Lowest temperature, Wind speed, Air pressure, Precipitation	Model inputs	China National Meteorological Science Data Service Network, ERA5-Land
Soil data	Gravel, Sand, Silt, Clay, Bulk, Organic	Gravel, Sandy soil, Silt, Clay, Organic matter content, Soil bulk density	Model inputs	World Soil Database (HWSD)

All spatiotemporal preprocessing is conducted on the Google Earth Engine (GEE) platform. To improve the reliability of the analysis, three filtering criteria are applied: (1) yield statistics must be available for at least two-thirds of the study period for each county; (2) counties in which maize planting accounts for less than 20 % of total land area are

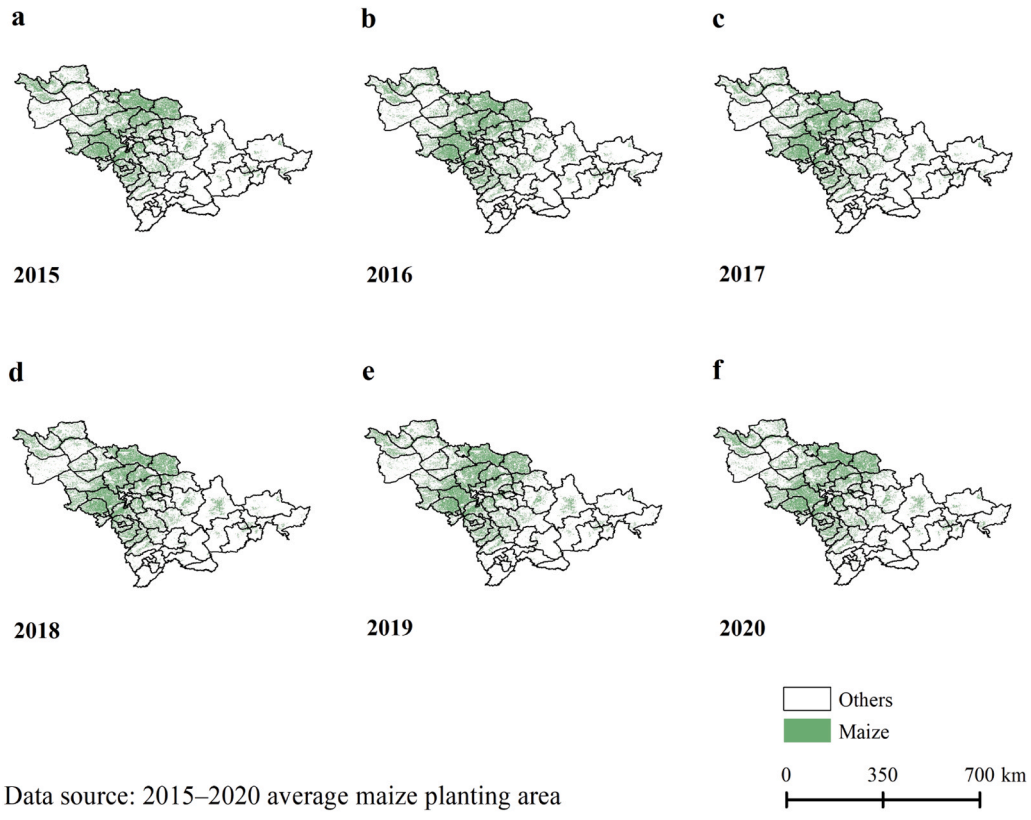


Fig. 2. Annual mean spatial distribution of maize planting in Jilin Province during 2015–2020.

excluded to ensure sample representativeness; and (3) counties for which the linear trend between yield and year is not statistically significant are removed. After these criteria are applied, 43 major maize-producing counties are retained as the study area (Féret et al., 2017; Sun et al., 2022).

Given the spatial heterogeneity of maize-growing environments in Jilin Province, accumulated temperature and maize yield data (Fig. 3a and 3b) are used to perform unsupervised k-means clustering. After non-representative counties are removed, effective regional delineation of major maize production zones is achieved, as shown in Fig. 3c. As illustrated in Fig. 3d and 3e, substantial differences in accumulated temperature and yield are observed between the eastern and western regions. Although Region 1 exhibits lower accumulated temperature, it maintains relatively high yield levels. This difference may be associated with spatial precipitation patterns: under rainfed conditions, growing-season precipitation generally decreases from east to west, a distribution that aligns with the higher productivity observed in Region 1.

2.3.2. *Meteorological sequence similarity matching*

Meteorological variables such as maximum temperature, minimum temperature, precipitation, vapor pressure, and wind speed are typical time-series data. Dynamic Time Warping (DTW) is a similarity-measurement method for time series; it adjusts the alignment between different time points within two sequences to identify an optimal matching path, thereby providing a more accurate assessment of their similarity (the DTW algorithm is described in Text S3). In this study,

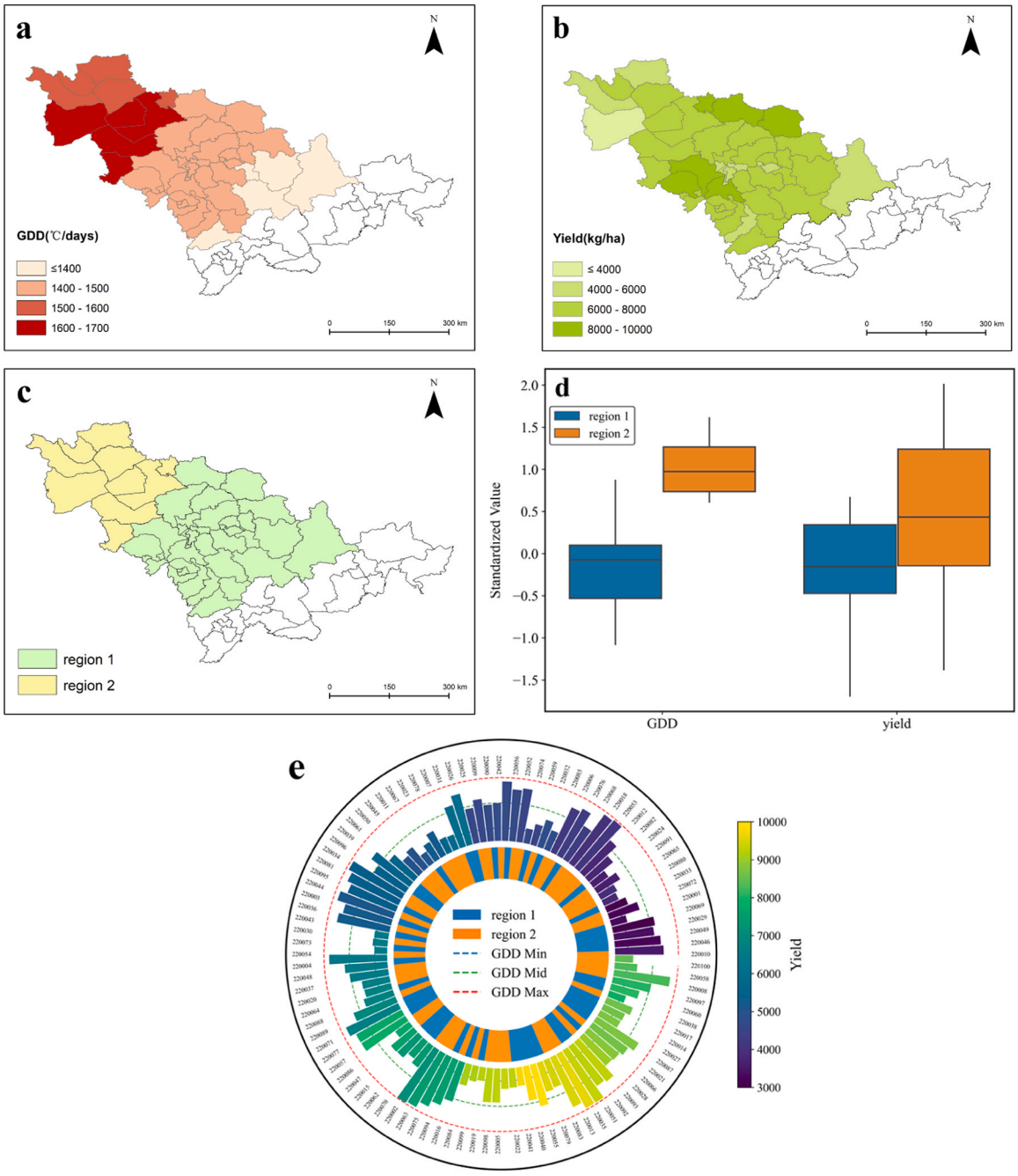


Fig. 3. County-level average maize yield and regional division in Jilin Province from 2015 to 2020. a shows the average accumulated temperature; b shows the average maize yield; c presents the regional division results; d compares the distribution of accumulated temperature and yield across regions; e illustrates the clustering of counties based on accumulated temperature and yield.

historical meteorological records from 1980 to 2014 are selected as the candidate set. The multivariate daily meteorological sequence of the target year prior to the forecast date (including Tmax, Tmin, PRECP, Vap, and Wind) is compared with all equal-length segments from each year in the candidate set by computing the cumulative DTW distance. The three years with the smallest distances are identified as the most similar years. Using the forecast date as the stitching point, the observed meteorological sequence of the target year before the forecast date is combined with the daily-mean sequences of the three similar years after the forecast date, resulting in a complete meteorological sequence for the target year.

2.4. Hybrid modeling approach

2.4.1. PROSAIL model

The PROSAIL model is a physically based canopy reflectance simulation tool that couples the PROSPECT model at the leaf level with the SAIL model at the canopy level (Rivera et al., 2013; Jay et al., 2017; Sinha et al., 2020). Its core mechanism involves using leaf reflectance and transmittance outputs from PROSPECT as inputs to the SAIL model, along with canopy structural parameters and observation geometry. Based on the radiative transfer equation, SAIL simulates the multiple scattering and reflection of light within the canopy, generating directional reflectance spectra. This integration enables physically consistent reconstruction of vegetation spectral responses across different wavelengths and observation conditions, providing a reliable basis for remote sensing inversion and crop parameter estimation. The main parameters of the PROSAIL model are listed in Table S1.

2.4.2. WOFOST model

The WOFOST (World Food Studies) model is a dynamic simulation system constructed based on crop physiological processes and ecological response mechanisms. Under various meteorological and soil conditions, it dynamically simulates photosynthesis, respiration, transpiration, and the accumulation and distribution of dry matter throughout the entire growing season (De Wit et al., 2019; Ceglar et al., 2019; Van Diepen et al., 1989). The model estimates daily assimilation rates and dry-matter production according to crop developmental progress and changes in leaf area, and allocates assimilates to different organs to simulate yield formation. The WOFOST model has been integrated into the Python Crop Simulation Environment (PCSE), enabling efficient coupling with multi-source data and flexible adjustment of model parameters, thereby enhancing its applicability in crop yield forecasting and agricultural decision support. In the regional-scale simulations conducted in this study, a unified baseline configuration is adopted: the model runs under rainfed conditions, and nitrogen is set as non-limiting. Site-level management information is used only to constrain phenology and initial states and to perform consistency checks, without being extrapolated to county-level grid cells, so as to avoid spatial bias that could arise from representing an entire county with a small number of stations and to ensure reproducibility. The main parameters of the WOFOST model are listed in Table S2.

2.4.3. Radiative transfer model coupled with machine learning

The traditional PROSAIL radiative transfer model, due to its clear physical mechanisms and strong interpretability, has been widely used for remote sensing-based inversion of leaf area index (LAI) (Alam et al., 2024; Jiao et al., 2021; Chen et al., 2022). However, the model relies heavily on prior parameterization and is sensitive to input variables, which limits its stability and applicability under complex surface conditions or across different regions (Féret et al., 2017; Sun et al., 2022). In recent years, machine learning algorithms have demonstrated strong nonlinear modeling capabilities, enabling the effective capture of complex relationships between remote sensing data and LAI. When sufficient training data are available, these methods offer higher predictive accuracy and modeling efficiency. Consequently, the integration of physical models with machine learning approaches—forming hybrid LAI inversion frameworks that combine physically based and data-driven strategies—has emerged as a promising direction to improve both the accuracy and generalizability of LAI retrieval.

2.4.4. Crop growth model data assimilation

By assimilating remote-sensing observations into a process-based crop growth model, the capability of the model to represent vegetation physiological status at the regional scale is enhanced. Compared with using the crop model alone, data assimilation optimizes the model state trajectory while maintaining biophysical consistency, thereby increasing agreement between model outputs and observations. In this study, the ensemble Kalman filter (EnKF) is employed to assimilate the retrieved leaf area index (LAI) into the WOFOST model, sequentially correcting model states and effectively enhancing the adaptability and accuracy of maize yield simulations in Jilin Province (Jiang et al., 2014; Wu et al., 2021; Dong et al., 2022). To ensure reproducibility, a 16-day assimilation interval is adopted and an ensemble size of $N = 100$ is used (sensitivity of ensemble members is shown in Fig. S1). The observation error standard deviation is set as a 10 % relative error, and the observation error covariance matrix R is represented in a diagonal form (Pan et al., 2019). A 10 % Gaussian perturbation is applied to parameters and initial states (sensitive parameters are listed in Section 3.2.1), with perturbations constrained within physiologically reasonable ranges (Huang et al., 2016). The assimilation framework is detailed in Text S2.

2.4.5. Hybrid model framework

A high-performance hybrid modeling framework is developed in this study for county-level maize yield prediction (Fig. 4). The framework integrates assimilated crop model outputs with multi-source observational data, incorporating five categories of predictive features: (1) Crop model predictors, derived by constructing a target-year substitute weather series using the dynamic time warping (DTW) algorithm and assimilating LAI to optimize WOFOST simulations, thereby generating crop growth model outputs; (2) Meteorological dynamic factors, including growing degree days (GDD), vapor pressure (vap), and wind speed (wind), to represent the climatic background during crop development; (3) Extreme weather indicators, calculated based on daily maximum and minimum temperatures and precipitation to derive heat stress accumulation (KDD), cold stress accumulation (FDD), and extreme precipitation amount (EPA), which reflect potential yield stress risks; (4) Growth status indicators, with NDVI employed as a biophysical proxy for canopy condition and photosynthetic capacity; and (5) Geographical and environmental factors, incorporating spatial location and soil properties to account for regional environmental heterogeneity. To enhance the representational capacity of heterogeneous data, appropriate statistical features are extracted by category: for meteorological and extreme weather indicators, 10-day cumulative values are used, while 10-day averages are calculated for crop model outputs, growth status indicators, and geographical–environmental variables.

In terms of model design, the hybrid framework (ENKF-WOFOST + CNN-ALSTM-MTL) consists of three key modules: an input module, a feature extraction module, and a region-specific output module (Fig. 5). Temporal data are processed by the CNN-ALSTM network to extract temporal features, whereas static data are processed by an MLP to extract static features. After the two types of features are extracted, they are fused and fed into a multi-task learning structure, where region-specific output layers generate county-level maize-yield estimates for each region. For the structural configuration, the CNN module employs 16 convolutional kernels with a kernel size of 3, a stride of 1, padding of 1, and the ReLU activation function to enhance nonlinear representation, followed by a max-pooling layer to reduce overfitting. The LSTM component consists of two stacked layers with 32 units each. A temporal attention layer is introduced after the LSTM: a single fully connected layer is used to obtain normalized weights for each time step in the sequence, and the hidden features of the entire sequence are weighted-

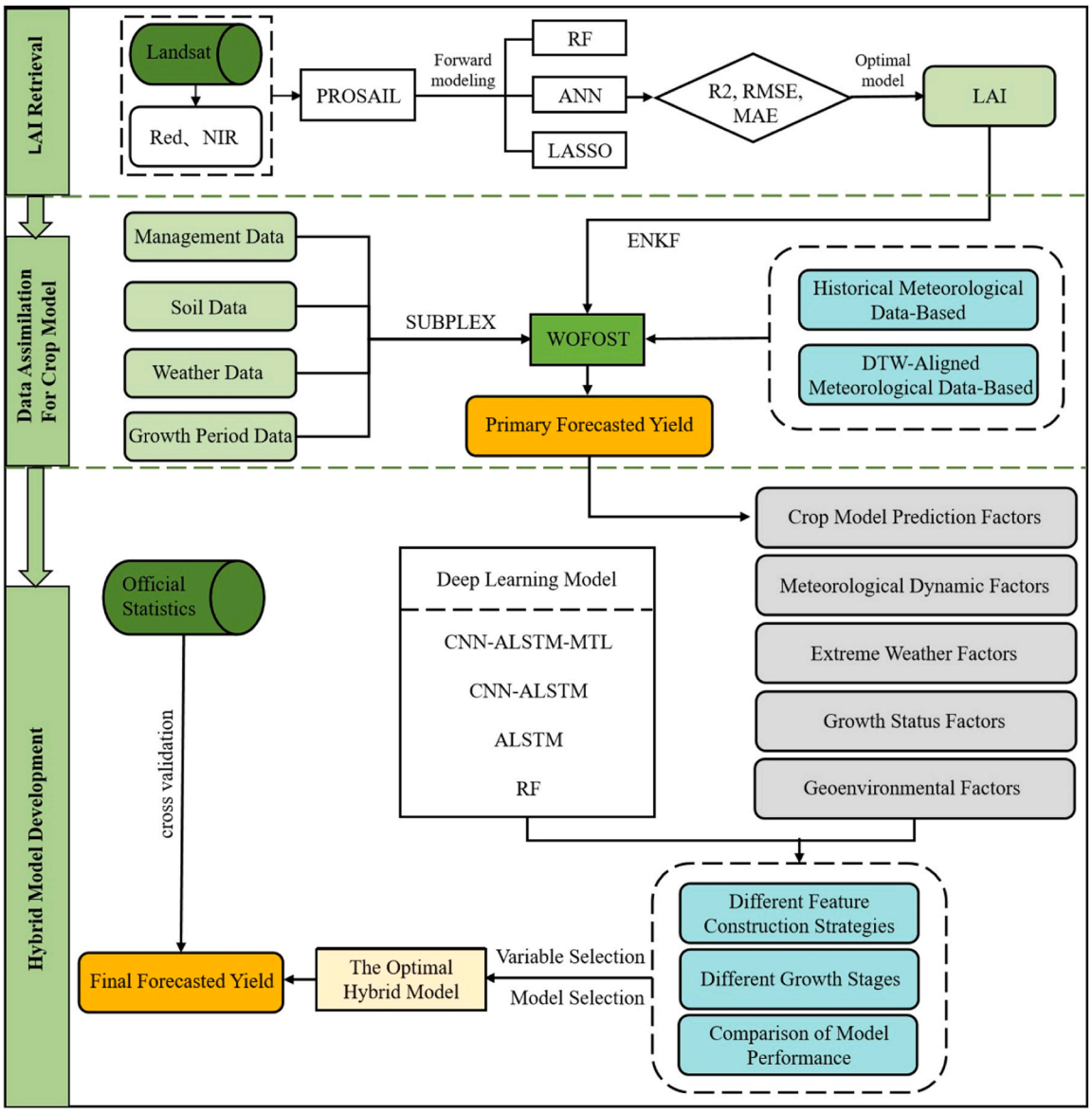


Fig. 4. Yield prediction framework.

aggregated to obtain the "weighted sequence features." This design avoids relying solely on the final time step and alleviates information decay in long sequences (see the Attention layer in Text S4 for details). The static-input branch adopts a two-layer MLP structure to extract features, with 32 neurons in each layer, for mining information from static variables. The output of the feature extraction module is formed by concatenating the temporal features extracted by the CNN-ALSTM network with the static features extracted by the MLP, generating a fused vector that serves as the input to the subsequent region-specific yield-estimation module. In the multi-task learning structure, the feature extraction module is shared across regions, whereas independent output layers are designed for each region at the output end to retain regional specificity. Detailed descriptions of each model layer are provided in Text S4.

In terms of training configuration, the following settings are adopted. A dropout rate of 0.2 is applied to the convolutional and temporal branches, and a dropout rate of 0.3 is applied to the static branch, together with L2 regularization (5×10^{-4}). Six-fold cross-validation is implemented by year (five years for training and one year for validation in each fold) to avoid temporal information leakage. During training, the validation-set RMSE is used as the monitoring metric. The maximum number of training epochs is set to 300, and early stopping is triggered when the validation-set RMSE shows no substantial decrease for 15 consecutive epochs, after which the model is restored to the weights that achieve the best validation performance. The optimizer is set to Adam (with a learning rate of 5×10^{-4}), the loss function is mean squared error (MSE), and the batch size is set to 16. Model training is conducted on a Windows 10 operating system using an Intel Core i7–10700 processor, 64 GB RAM, and an NVIDIA GeForce RTX 3080 GPU (10 GB GDDR6X), with PyTorch as the deep-learning framework.

2.5. Model evaluation and metrics

Three models—RF, ALSTM, and CNN-ALSTM—are used as baselines to compare and evaluate the performance of the CNN-ALSTM-MTL model in maize-yield estimation. The RF model, as a widely applied representative of tree-based approaches, serves as a reference for non-temporal modeling. The CNN-ALSTM model is structurally similar to CNN-ALSTM-MTL but does not incorporate a multi-task learning mechanism, making it unable to capture inter-regional differences; therefore, it is used as a comparative model to examine whether regional partitioning contributes to improving estimation accuracy. To evaluate

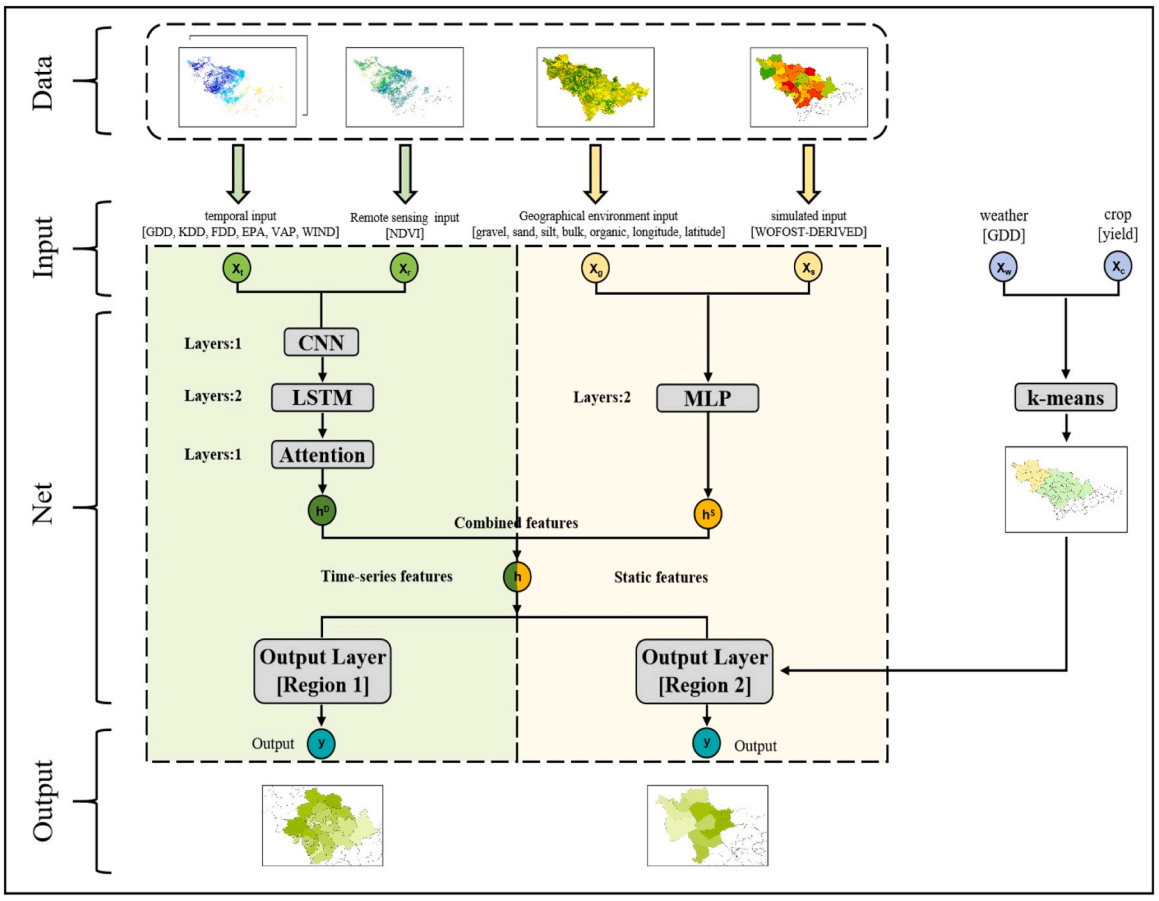


Fig. 5. Architecture of the CNN-ALSTM-MTL model.

the performance of the assimilated crop model and the hybrid modeling framework, three widely used metrics in predictive analysis are selected: root mean squared error (RMSE), coefficient of determination (R^2), and mean absolute error (MAE). All metrics are computed based on the "county × year" samples, where the labels correspond to county-level statistical yield. The calculation formulas are as follows:

$$R^2 = 1 - \frac{\sum_{i=1}^{m}(O_i - S_i)^2}{\sum_{i=1}^{m}(O_i - \overline{O})^2} \quad (1)$$

$$RMSE = \sqrt{\frac{1}{m}\sum_{i=1}^{m}(O_i - S_i)^2} \quad (2)$$

$$MAE = \frac{1}{m}\sum_{i=1}^{m}|O_i - S_i| \quad (3)$$

where O_i is the actual yield in county i, S_i is the predicted yield in county i, O is the mean of the observed values, and m is the number of counties.

3. Results

3.1. LAI inversion results based on the PROSAIL model

3.1.1. Sensitivity analysis of PROSAIL model parameters

Accurately determining the type and number of PROSAIL parameters is essential for reliable LAI inversion. Including parameters with low sensitivity unnecessarily can introduce noise into the subsequent machine learning training process, thereby obscuring the variables that play a decisive role in LAI estimation. To address this, hyperspectral reflectance simulated by PROSAIL is converted into multispectral reflectance consistent with Landsat-8 OLI spectral bands using spectral response functions, and the red (Red) and near-infrared (NIR) bands are selected for LAI inversion. EFAST sensitivity analysis (Fig. 6) identifies LAI, the soil brightness factor (Psoil), leaf dry-matter content (Cm), and the leaf inclination distribution function (LIDFA) as highly sensitive parameters that exert strong influence on reflectance variation. Although chlorophyll content (Cab) shows limited sensitivity outside the visible spectrum, it is retained as a free parameter due to its central role in plant photosynthesis, thereby enhancing the model's ability to represent actual vegetation physiological conditions.

3.1.2. Evaluation of the machine learning–coupled inversion algorithm

To ensure the accuracy and reliability of the inversion results, the performance of three mainstream machine-learning methods—random forest (RF), artificial neural network (ANN), and LASSO regression—is evaluated (method descriptions are provided in Text S5). PROSAIL model parameters are obtained using a genetic algorithm (population size of 50, crossover rate of 0.8, mutation rate of 0.1), and the model is forward-simulated to generate 100,000 paired samples of LAI and remote-sensing reflectance, which constitute the dataset for the machine-learning algorithms. Robust model evaluation is ensured through a cross-validation strategy, with 80 % of the samples used for training and 20 % used as the test set; field-measured data are incorporated to provide additional validation. Model accuracy is assessed using R^2, RMSE, and MAE (Fig. 7). The results show that the RF model achieves the highest performance in LAI inversion ($R^2 = 0.884$, RMSE = 0.505, MAE = 0.401), surpassing both ANN and LASSO regression. ANN provides satisfactory fits in the low-LAI range (<2) but exhibits systematic underestimation in the high-LAI range (>4) ($R^2 = 0.863$). LASSO shows comparatively lower overall accuracy ($R^2 = 0.845$). Owing to its superior predictive accuracy and generalization capability,

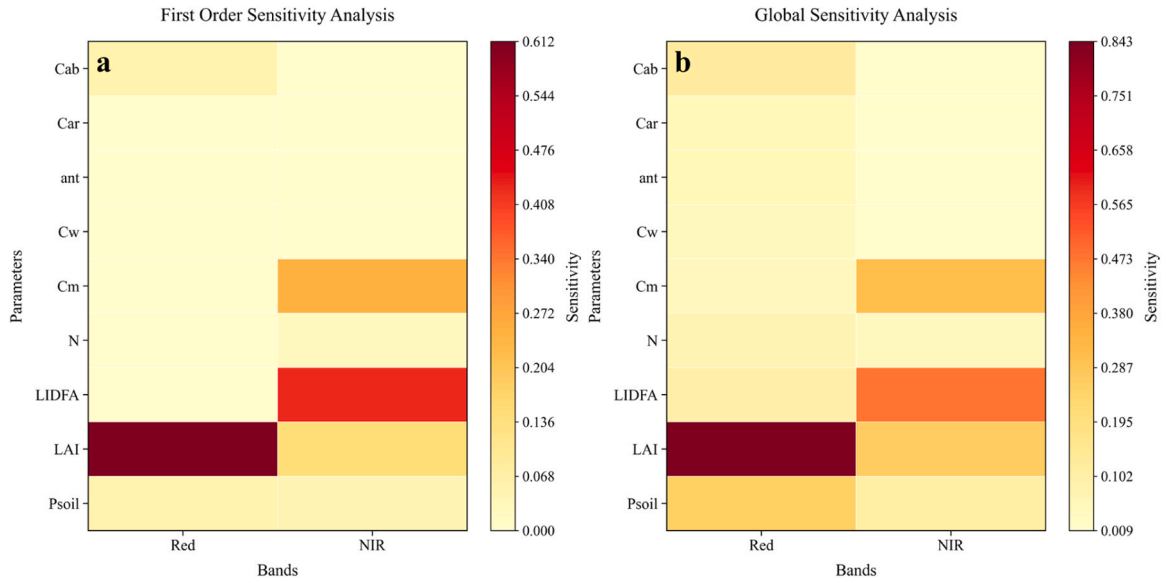


Fig. 6. Sensitivity analysis of PROSAIL model parameters. a shows the first-order sensitivity analysis; b shows the global sensitivity analysis.

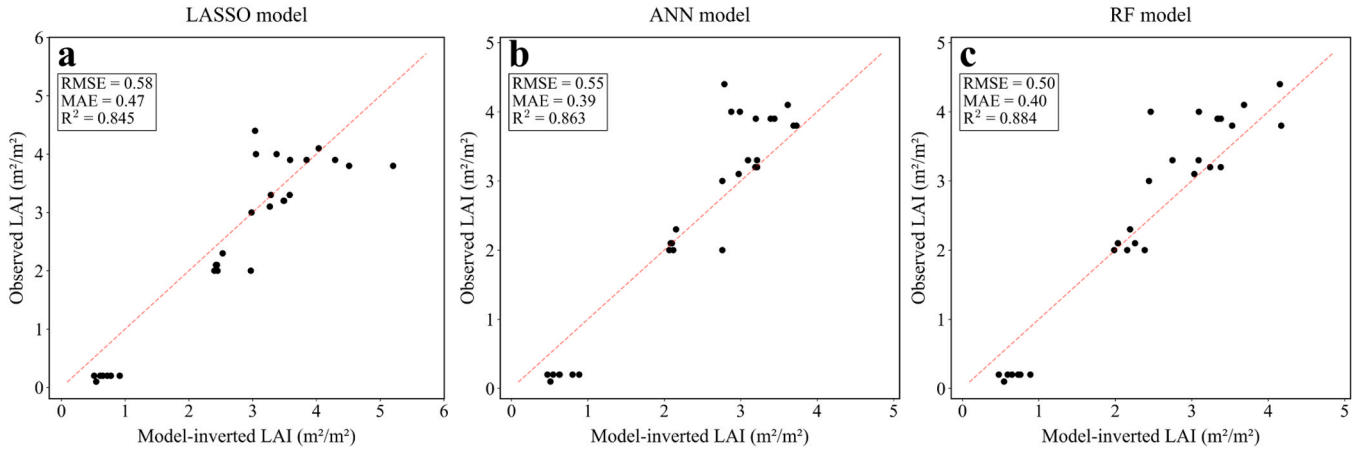


Fig. 7. Comparison between model-inverted LAI and ground-measured LAI.

the RF model is selected as the primary approach for LAI inversion across maize-growing areas in Jilin Province and is applied to pixel-scale LAI estimation across the entire region. Details of the key parameters and their determination procedures are provided in Text S5.

3.1.3. Regional accuracy assessment

To further evaluate the spatial performance of the machine learning model in estimating leaf area index (LAI), we conducted a systematic comparison between the LAI spatial distribution estimated by the optimal model across four maize growth stages (T1–T4) in Jilin Province and that derived from MODIS remote sensing products.

The results demonstrated a high level of agreement between the two datasets in most growth stages (Fig. 8). During the early T1 stage, MODIS LAI values were primarily distributed between 0.1 and 0.6, with the lowest values observed in eastern Jilin Province. The simulated LAI values exhibited a similar spatial pattern. In the T2 stage, MODIS LAI values mainly ranged from 0.6 to 1.2, and the model outputs generally aligned with this range, although localized overestimations of around 0.6 were identified in parts of central Jilin. The T3 stage corresponds to the rapid growth phase of LAI, during which both MODIS and model-estimated LAI values were concentrated between 2.4 and 4.2, indicating strong consistency. In the final T4 stage, MODIS LAI values were mostly between 1.8 and 3.6, whereas the model produced relatively higher estimates, primarily ranging from 2.4 to 4.2, resulting in a systematic overestimation of approximately 0.6 and indicating reduced inversion accuracy in this stage. According to the statistical analysis of pixel distribution ratios across the four stages, the error between model-derived LAI and MODIS LAI remained within 15 % for stages T1 to T3, while the discrepancy in T4 approached 20 %. Nevertheless, at the macro spatial scale, the spatial variation and distribution trends of LAI estimated by the optimal model remain largely consistent with those derived from MODIS across all growth stages.

3.2. Performance of the WOFOST model based on data assimilation

3.2.1. Sensitivity analysis of WOFOST model parameters

As part of the yield sensitivity analysis, the WOFOST model is systematically evaluated across different regions (Fig. 9a and 9b). A sensitivity threshold of 0.1 is applied. The results indicate a high level of consistency in the composition of dominant sensitive parameters across regions, particularly for those critical to yield determination. In Region 1, the most influential parameters include the initial dry weight of the crop (TDWI), specific leaf area (SLATB1), maximum assimilation rate (AMAXTB125), leaf lifespan (SPAN), maintenance respiration rate of aboveground organs (RMO), thermal time from flowering to maturity (TSUM2), accumulated temperature during the reproductive phase

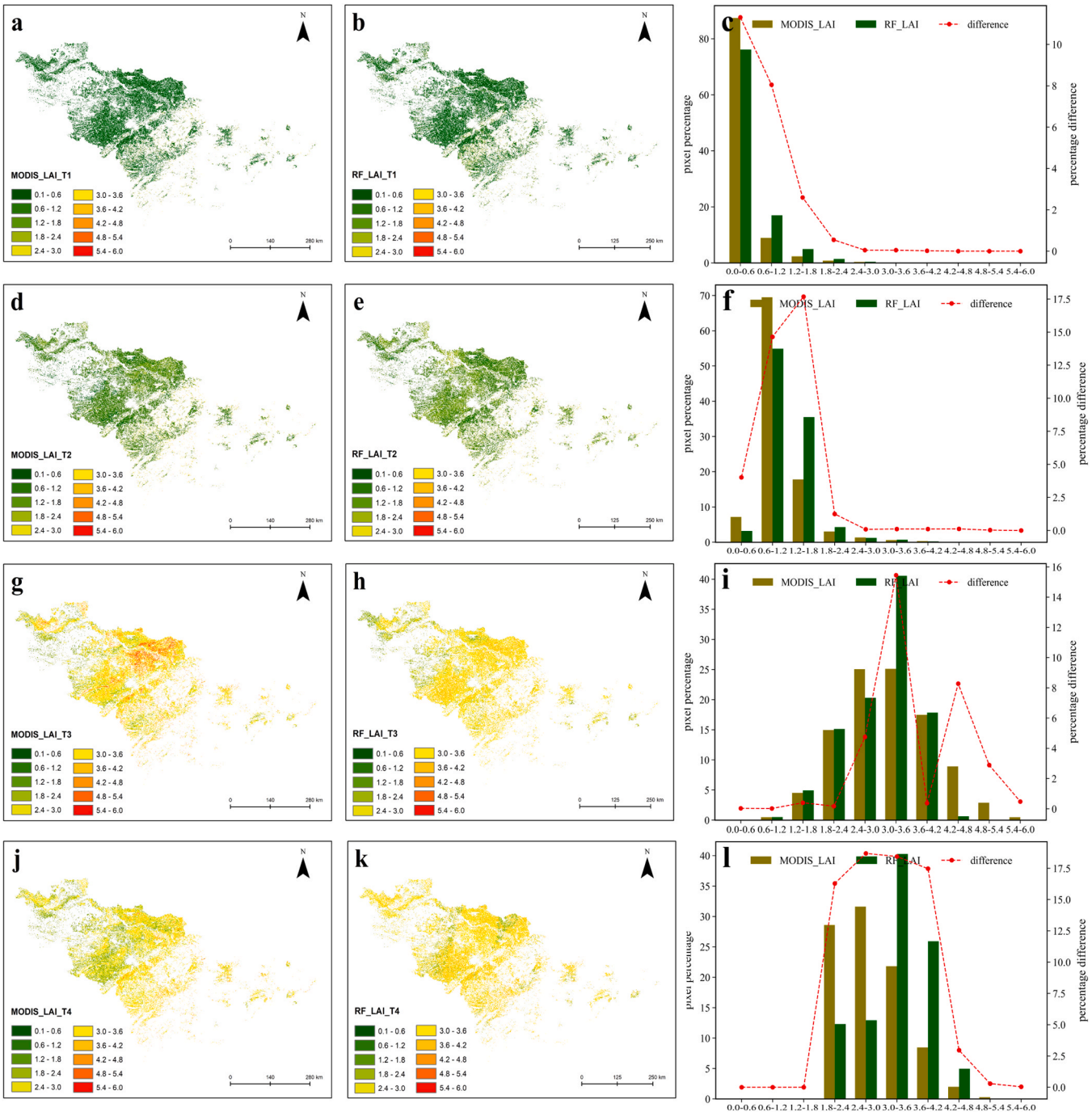


Fig. 8. Spatial distribution and interval statistics of the annual mean LAI across different growth stages from 2015 to 2020. a, d, g, and j show the spatial distribution of MODIS-derived LAI; b, e, h, and k show the spatial distribution of model-estimated LAI; c, f, i, and l present interval-based statistical comparisons between MODIS and model-estimated LAI.

(TSUM1), and relative growth rate (CVS). These parameters exhibit substantial impacts on model outputs. Notably, TSUM2 and RMO show sensitivity indices approaching 0.5 in both regions, highlighting the central role of temperature accumulation and respiratory cost in yield formation. In Region 2, beyond the parameters shared with Region 1, three additional secondary sensitive factors are identified: stem maintenance respiration rate (RMS), maximum assimilation rate under stomatal opening conditions (AMAXTB0), and root conversion efficiency of assimilates (CVR). These parameters exhibit relatively low sensitivity indices, around 0.1, which may result from differences in regional agricultural management practices that elevate the influence of otherwise non-sensitive parameters. Despite these variations, the composition of the most sensitive parameters remains largely consistent between the two regions.

As a dynamic process-based model operating on a daily time step, the WOFOST model requires sensitivity analysis of state variables throughout crop development due to its continuous simulation nature. Sensitivity analysis of the leaf area index (LAI) across different growth stages of spring maize in Jilin Province (Fig. 9c–9f) reveals distinct temporal patterns in the response to model parameters. During the emergence to jointing stage, LAI is most sensitive to the initial dry matter (TDWI) and the specific leaf area growth rate (SLATB), indicating that early canopy establishment is primarily governed by initial biomass and leaf expansion capacity. In the jointing to tasseling stage, the base

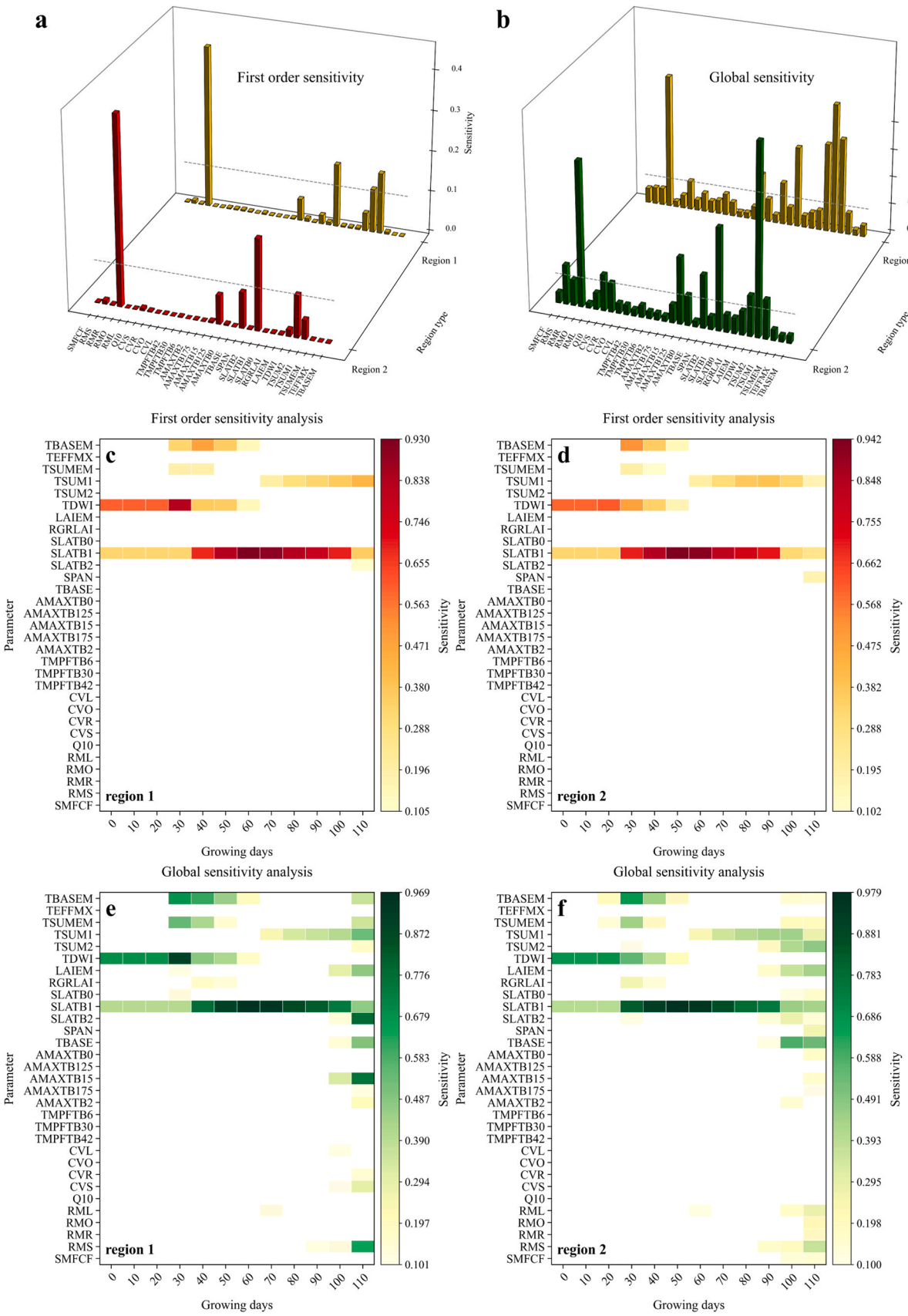


Fig. 9. Sensitivity indices of yield and leaf area index across growth stages. a shows the first-order sensitivity analysis of yield in different regions; b shows the global sensitivity analysis of yield in different regions; c and d show the first-order sensitivity analysis of leaf area index in different regions; e and f show the global sensitivity analysis of leaf area index in different regions.

temperature (TBASEM) and the thermal time required for vegetative growth (TSUMEM) serve as the dominant drivers, reflecting the crop's strong dependence on thermal conditions during this developmental phase. From tasseling to grain-filling, TSUM1 emerges as the leading variable, highlighting the influence of early reproductive-stage temperature accumulation on structural development during this period. In the grain-filling to maturity stage, model sensitivity becomes more complex, with maximum photosynthetic efficiency (AMAXTB15), root biomass (RMS), and the LAI establishment coefficient (LAIEM) identified as key parameters. These results underscore the reliance of yield formation in this stage on sustained leaf functionality and efficient assimilate transport. Overall, the analysis not only reveals the stage-specific influence of different parameters but also provides a precise basis for variable selection in subsequent data assimilation and model calibration efforts.

3.2.2. *Evaluation of the model after assimilation*

In this study, the SUBPLEX algorithm is first used to optimize the highly sensitive parameters of the WOFOST model to improve the initial simulation accuracy (Fig. 10a). On this basis, the Ensemble Kalman Filter (ENKF) is introduced to further enhance model performance through data assimilation. Fig. 10a presents the model's yield prediction performance without assimilation, while Fig. 10c shows a marked improvement in accuracy after incorporating ENKF. To more accurately evaluate the assimilation effect, historical meteorological observations are used as model inputs. As shown in Fig. 10b, without assimilation, the model tends to overestimate maize yield in low-yielding areas (3000–6000 kg/ha) and underestimate it in high-yielding areas (6000–7000 kg/ha). Notably, near 6500 kg/ha, a deviation of approximately 7 %age points is observed between simulated and measured values, indicating limited performance in capturing yield extremes. In contrast, Fig. 10d demonstrates that the consistency between simulated and observed yields significantly improves after assimilation. Specifically, 60.4 % of counties have a prediction error below 10 %, 35.4 % fall within 20 %, and only 4.2 % exceed a 20 % error threshold. The overall model evaluation metrics show a root mean square error (RMSE) of 730.54 kg/ha, a mean absolute error (MAE) of 584.69 kg/ha, and a coefficient of determination (R^2) of 0.591. These results demonstrate that by optimizing model states through ENKF, the gap between simulated and observed values is effectively reduced, thereby enabling more accurate simulation of maize growth and development. To assess improvements in intermediate crop growth processes resulting from assimilation, the leaf area index (LAI)—a key physiological state variable in WOFOST—is selected for comparison using actual observations. A marked enhancement is observed in the consistency between simulations and observations after assimilation (a 21 % increase in R^2 and a 34 % decrease in RMSE), thereby providing mechanistic support for the improved yield accuracy (Fig. S2).

3.2.3. *Construction of DTW-based meteorological sequences and stage-specific yield prediction performance for the target year*

To validate the applicability of DTW-selected meteorological data for driving the WOFOST model across maize growth stages, the fitting accuracy and assimilation performance of the selected data are evaluated in detail. A comparison between the DTW-selected similar years for each stage (T1–T4) and the actual meteorological observations during the target years (2015–2020) shows that the reliability of the substitute data improves progressively over time, with the highest accuracy observed at T3 and T4. As shown in Fig. 11a, the correlation coefficient for minimum temperature at T4 approaches 0.8, while maximum temperature exceeds 0.6—substantially higher than the dispersed correlations in T1 and T2. These findings indicate that during later growth stages, when

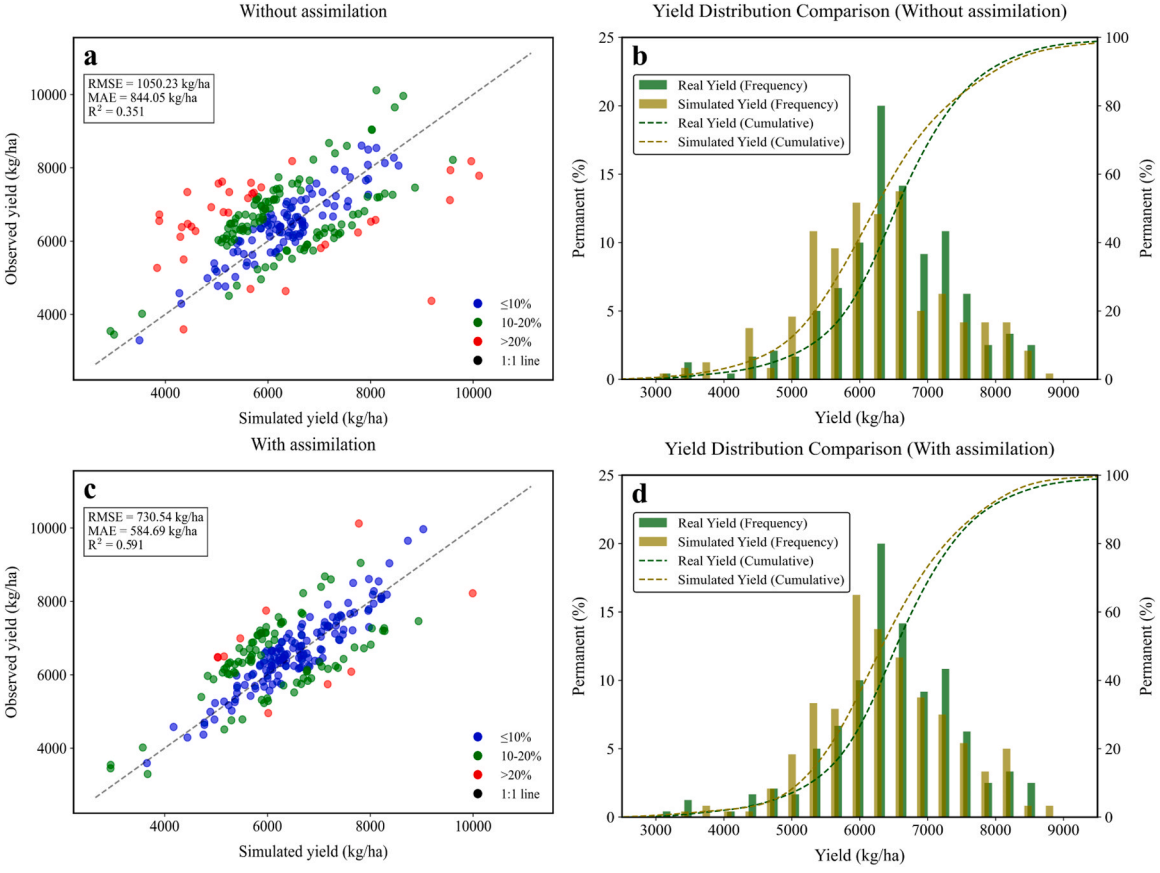


Fig. 10. Comparison of Simulated and Observed Maize Yields at the County Scale. a and b show yield predictions after model calibration but before data assimilation; c and d show yield predictions after data assimilation.

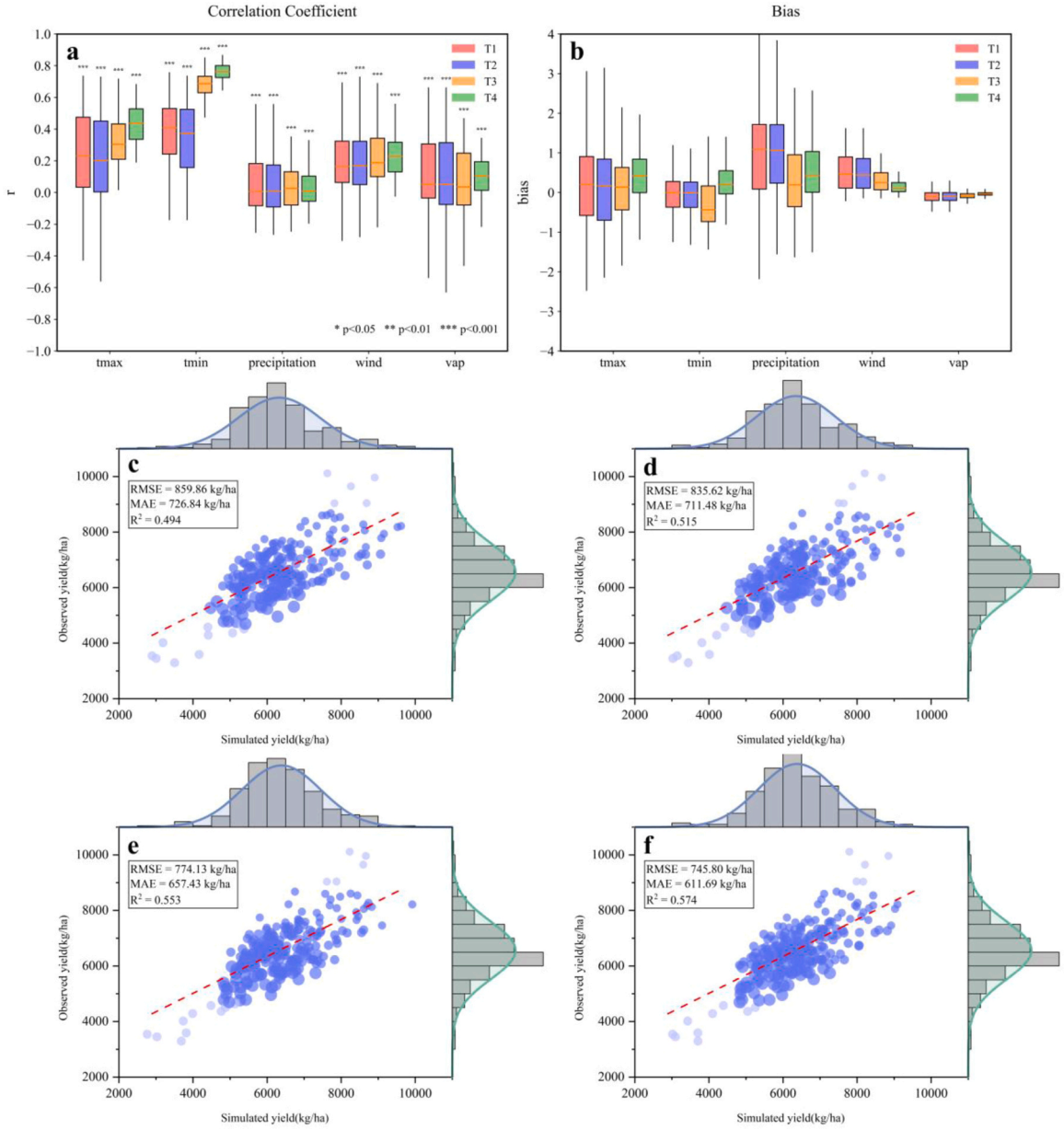


Fig. 11. Meteorological matching and county-level yield prediction based on the DTW algorithm. a and b present the evaluation of weather similarity using the DTW algorithm; c, d, e, and f show yield predictions for each growth stage.

meteorological conditions become more stable, DTW-selected historical sequences more accurately capture the actual variability of the growing season. In contrast, precipitation exhibits lower correlations, likely due to its inherent spatiotemporal variability, observational uncertainty, and associated statistical dispersion. Bias analysis (Fig. 11b) further confirms this trend: deviations in Tmax and Tmin during T3 and T4 are narrow, remaining within ±1, while biases in wind speed and vapor pressure converge toward zero, indicating more accurate estimation of meteorological variables at the overall scale. Collectively, the superior performance of T3 and T4 highlights that the meteorological data selected for these stages outperform those for earlier stages in both correlation and error control, exhibiting stronger reliability and representativeness. This also confirms the feasibility of using substituted meteorological data for future-season prediction, and the comparison with the multi-year mean of the observed meteorological data is shown in Fig. S3. In addition, variance homogeneity tests (Levene and Brown–Forsythe, $\alpha = 0.05$) were conducted for each meteorological variable at the stitching points of the DTW-constructed sequences to verify whether the amplitude of variability remains consistent before and after sequence stitching ($p \geq 0.05$ indicating homogeneous variance). Apart from precipitation, which shows $p < 0.05$ in a small number of county–year stage units (approximately 2.3 %), all other variables generally satisfy the homogeneity requirement, as shown in Fig. S5.

To further evaluate the performance of DTW-generated meteorological sequences in yield prediction, data assimilation is applied to the WOFOST model using observations from different growth stages, and a "multi-year mean meteorology" control group is added and compared in parallel with the DTW-generated sequence. During T1–T2 (Fig. S4), the differences between the two groups are small (with DTW performing slightly better), whereas during T3–T4, the DTW group shows an average increase of 0.03 in R^2 (+5.62 %) and a reduction of 40.5 kg/ha in RMSE (−5.06 %) relative to the multi-year mean meteorology. Fig. 11c–11f show that assimilation progressively improves prediction accuracy as real-time meteorological and observational information accumulates. At T1, limited meteorological observations and sparse LAI retrievals introduce uncertainty into the DTW-based meteorological

sequence, resulting in relatively low prediction accuracy after assimilation. As the growth stages progress, more data are obtained during T2–T3, leading to a marked improvement in prediction accuracy of approximately 7 %. By T3 and T4, the model's yield predictions align closely with simulations driven by complete historical meteorological data (Fig. 10c), demonstrating strong reliability and predictive potential. Therefore, compared with the multi-year mean meteorology, the DTW-constructed target-year meteorological sequence better preserves its temporal variation pattern and maintains assimilation accuracy when early-season information is insufficient.

3.3. Prediction performance of the hybrid model under different feature construction strategies

According to previous studies, traditional hybrid models rely on crop model outputs driven by historical meteorological data as input features (Feng et al., 2019; Jeong et al., 2022). An improved feature construction strategy is proposed by incorporating the Dynamic Time Warping (DTW) algorithm, which identifies the historical year most similar to the target year based on meteorological sequence similarity during the growing season. Meteorological data from the selected historical year are then combined with real-time observations from the target year to generate a complete meteorological sequence for simulating that year's crop growth process.

Using this enhanced feature strategy, a comprehensive ENKF-WOFOST+CNN-ALSTM-MTL framework is developed that integrates multisource heterogeneous data, including remote sensing indices, meteorological variables, crop physiological traits, soil parameters, and geographic environmental factors. To address the challenge of missing future meteorological data, we developed two feature construction strategies: one based on WOFOST assimilation-historical meteorological-driven features (Fig. 12a), and the other based on WOFOST assimilation-DTW-screened meteorological-driven features (Fig. 12b). The latter approach enables more representative weather inputs for the target year by selecting historically similar meteorological patterns, thereby supporting the WOFOST model in generating more accurate predictions of physiological parameters.

Experimental results show that the DTW-based strategy (Strategy 2) outperforms the historical meteorology-based strategy (Strategy 1). In maize yield predictions across Jilin Province, this method achieves a coefficient of determination (R^2) of 0.811, with a root mean square error (RMSE) of 565 kg/ha and a mean absolute error (MAE) of 435 kg/ha—representing an approximate 5 % improvement in prediction accuracy compared to conventional methods. In future work, integrating ensemble-based probabilistic forecasts from multiple weather prediction products may allow the model to learn from both historical and forecasted patterns, enhancing its ability to quantify uncertainty and generate more robust yield predictions.

3.4. Analysis of the optimal prediction stage

To enable early forecasting of maize yield and to determine the optimal prediction window, a hybrid model is constructed using Feature Strategy 2 as input variables, based on the analytical conclusions presented in Section 3.3. The model's performance is systematically evaluated across different growth stages (T1–T4). As shown in Fig. 13, prediction accuracy steadily improves as crop development progresses, with the most significant gains observed between stages T1 and T3: the coefficient of determination (R^2) increases by approximately 40 %, while the root mean square error (RMSE) decreases by about 26 %. This trend suggests that, with the continuous accumulation of meteorological and crop growth information, the model captures growth dynamics more effectively, thereby enhancing prediction accuracy. However, the performance improvement becomes marginal from T3 to T4, indicating that the model approaches a performance plateau. Stage T3 (jointing to tasseling stage) represents a critical period characterized by peak photosynthetic activity and rapid biomass accumulation, which lays the foundation for grain formation. During this phase, maize is particularly sensitive to environmental conditions, making the input data at T3 highly representative for predictive modeling, a physiological basis that is further elaborated together with supporting data evidence in Section 4.1. In contrast, although a slight improvement is still observed in T4 (tasseling to maturity stage), the rate of increase diminishes. This may be attributed to the reduced sensitivity of grain filling and maturation processes to external environmental fluctuations, as well as the stabilization of certain physiological parameters, which limits the added value of new input information. Considering both the timeliness and performance of prediction, stage T3 offers a favorable balance by providing forward-looking insight while still allowing sufficient lead time for early intervention and decision-making.

3.5. Performance evaluation of the hybrid model

Based on the analysis in Section 3.4, the T3 simulation period is used to compare the performance of four models—RF, ALSTM, CNN-ALSTM, and CNN-ALSTM-MTL—in predicting maize yield in Jilin Province. In terms of model architecture, the CNN-ALSTM-MTL model incorporates a multi-task learning mechanism to capture cross-regional yield differences, allowing it to better represent regional heterogeneity than single-task approaches and thereby improving generalization. As shown in Fig. 14a, CNN-ALSTM-MTL achieves the highest accuracy under six-fold cross-validation, with an average RMSE of 592 kg/ha and an average R^2

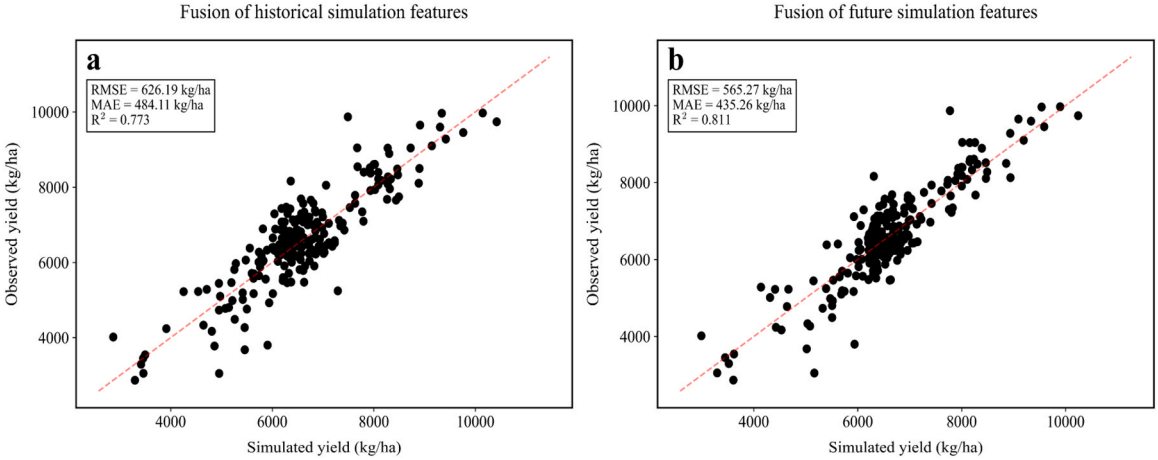


Fig. 12. Model prediction performance under different feature construction strategies.

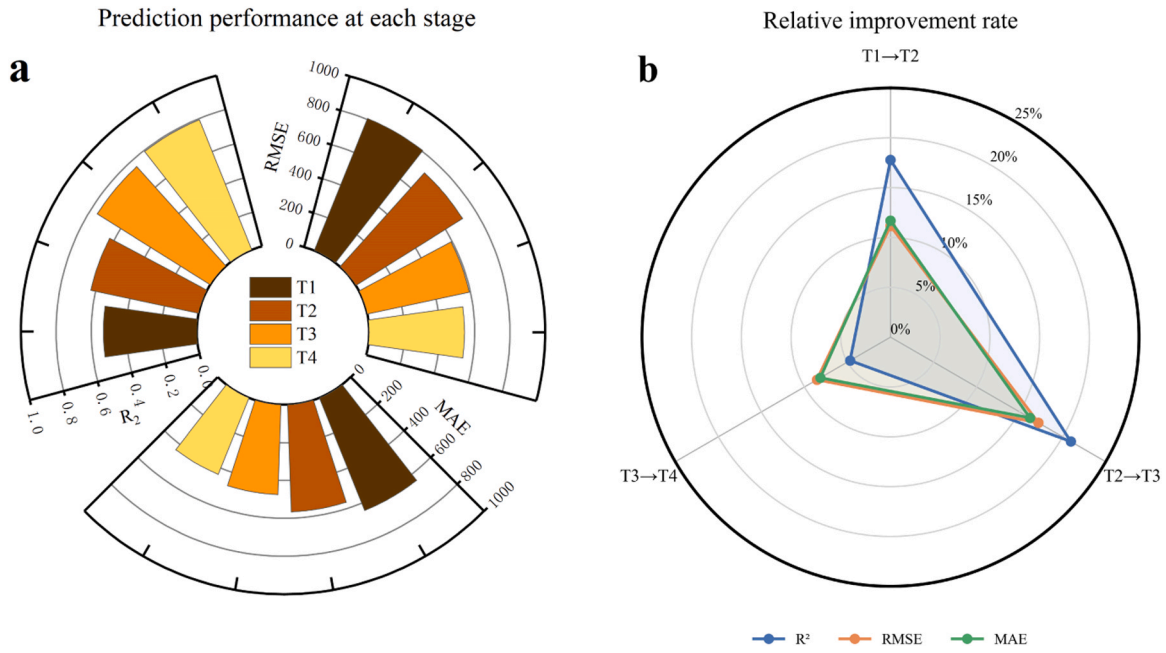


Fig. 13. Prediction performance of the model across different growth stages. a shows the prediction performance of the model at each growth stage; b presents the relative improvement rate of model performance across growth stages.

of 0.75 (Fig. 14b–14c). Relative to the RF model (RMSE = 661 kg/ha, R^2 = 0.66), the ALSTM model exploits the temporal-learning capability of long short-term memory networks to reduce the error to 640 kg/ha and raise R^2 to 0.70. Building on this, the CNN-ALSTM model integrates a one-dimensional convolutional neural network (1D-CNN) structure to extract spatial correlations in complex data, after which the LSTM captures their temporal dependencies, thereby improving predictive accuracy to an average RMSE of 624 kg/ha and an R^2 of 0.72. These findings align with earlier studies showing that convolutional neural networks effectively capture hierarchical spatial structures and enhance the representational capacity of models applied to complex inputs (Wang et al., 2021).

Under the framework of six-fold cross-validation, county-level maize yield estimates are evaluated using RMSE as the metric to assess each model's ability to capture the spatial distribution of yield (Fig. 15). Given the overall average RMSE of 592 kg/ha, an RMSE below 600 kg/ha is defined as the threshold for good performance. The CNN-ALSTM-MTL model demonstrates the best overall performance, with yield estimation errors remaining below 600 kg/ha in approximately 62 % of counties (Fig. 15d), indicating strong generalization capacity in capturing spatial heterogeneity of maize yield. In contrast, the RF model and the traditional ALSTM model exhibit RMSE values exceeding 600 kg/ha in about half of the counties (Fig. 15a and Fig. 15b), reflecting higher overall errors. Although the CNN-ALSTM model, which incorporates convolutional layers, partially alleviates this issue, its overall performance remains slightly inferior (Fig. 15d and Fig. 15e). Notably, all models yield relatively high RMSE values—exceeding 1000 kg/ha—for maize yield estimation in Erdao District of Changchun City. Further analysis reveals that this region exhibits a missing-data rate of approximately 30 %, confirming the important influence of sample size on model prediction accuracy (Benkendorf and Hawkins, 2020; Stockwell and Peterson, 2002). Future efforts will prioritize completing the missing annual records in the county statistical yearbooks to improve label coverage and reduce errors caused by sparse samples. Overall, the CNN-ALSTM-MTL model improves the accuracy of county-level maize spatial distribution estimation by effectively extracting spatiotemporal features and capturing spatial heterogeneity.

By evaluating the performance of multiple maize yield estimation models across different spatial regions, the advantages of regional partitioning combined with a multi-task learning approach are verified. The results show that the CNN-ALSTM-MTL model achieves the highest estimation accuracy in both regions, with the lowest RMSE and the highest R^2, outperforming the baseline CNN-ALSTM, ALSTM, and RF models. The performance trends of the models are consistent across the two regions. After the introduction of the multi-task learning mechanism, the CNN-ALSTM-MTL model improves average accuracy by approximately 3 % compared with the CNN-ALSTM model, with a particularly notable improvement in Region 1, where RMSE decreases from 680 kg/ha to 628 kg/ha—an 8 % reduction that reflects a clear optimization effect. Fig. 16c–16d further quantifies the improvements of CNN-ALSTM-MTL over the RF, ALSTM, and CNN-ALSTM models in both regions. Positive gains are achieved in both regions, with greater improvements observed in Region 1. Using ALSTM as the baseline, the R^2 improvement in Region 1 reaches 10.96 %, whereas the improvement in Region 2 is 1.77 %. Using CNN-ALSTM as the baseline, Region 1 exhibits an R^2 increase of 5.66 %, compared with 1.63 % in Region 2. In addition, ΔGap R^2 results indicate that CNN-ALSTM-MTL reduces the R^2 disparity between the two regions by 32.2 %, 17.4 %, and 33.4 % relative to the three baseline models, respectively, demonstrating its enhanced ability to mitigate inter-regional performance differences (calculation formulas are provided in Text S6). At the mechanistic level, the prediction results of the two regions (Fig. 16a–b) show that all models achieve higher accuracy in Region 2 than in Region 1. This difference is attributed to the flatter terrain and more standardized agricultural management practices in western Jilin Province compared with the eastern region, which provide more consistent and complete datasets. Previous studies have emphasized that data consistency and low noise are essential for deep learning models to extract stable spatiotemporal features (Cai et al., 2022). Consequently, the higher data quality and the relatively consistent crop growth environment in Region 2 enable the models to learn maize yield variability more effectively, resulting in better predictive performance in this region.

4. Discussion

4.1. Advantages of the hybrid model

This study proposes an innovative hybrid framework that integrates

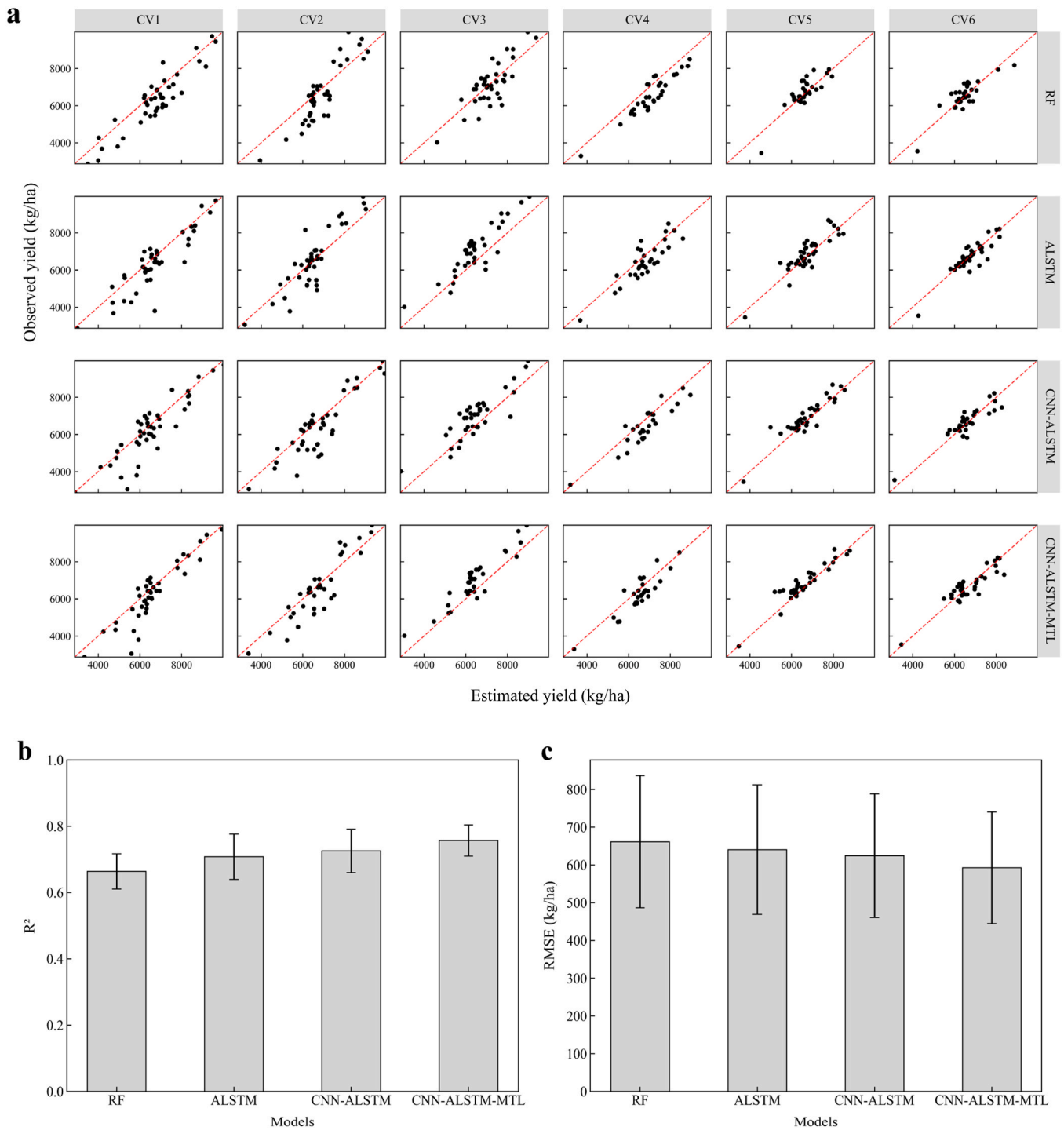


Fig. 14. Prediction performance of each model under six-fold cross-validation. a shows the scatterplot of predicted yield versus county-level yield; b shows the R^2 values for predicted versus county-level yield; c shows the RMSE values for predicted versus county-level yield.

remote-sensing data assimilation, process-based crop modeling, and deep learning techniques to substantially improve both the accuracy and timeliness of maize yield prediction. Table 2 summarizes representative crop-yield prediction studies conducted in recent years. The analysis shows that, although these studies have achieved notable progress, existing approaches still exhibit several limitations. For example, many maize-related studies tend to produce stable yield assessments only at the milk or grain-filling stage, whereas the present study delivers reliable predictions as early as T3 (jointing to tasseling stage), advancing the prediction window by approximately one growth stage. Methods 2 and 3 in Table 2 rely on remote sensing data from specific time points and lack a comprehensive consideration of temporal dynamics. However, crop development is a progressive and continuous process, during which environmental stress at different growth stages can cumulatively influence final yield. Therefore, accurately characterizing the biomass accumulation process is essential for understanding how crop yield is formed. (Li et al., 2023b; Ji et al., 2022). Methods 4–6 demonstrate the application of deep learning techniques. For example, Wang et al. apply LSTM networks to predict winter wheat yields in North China and find that incorporating soil characteristics improves model performance,

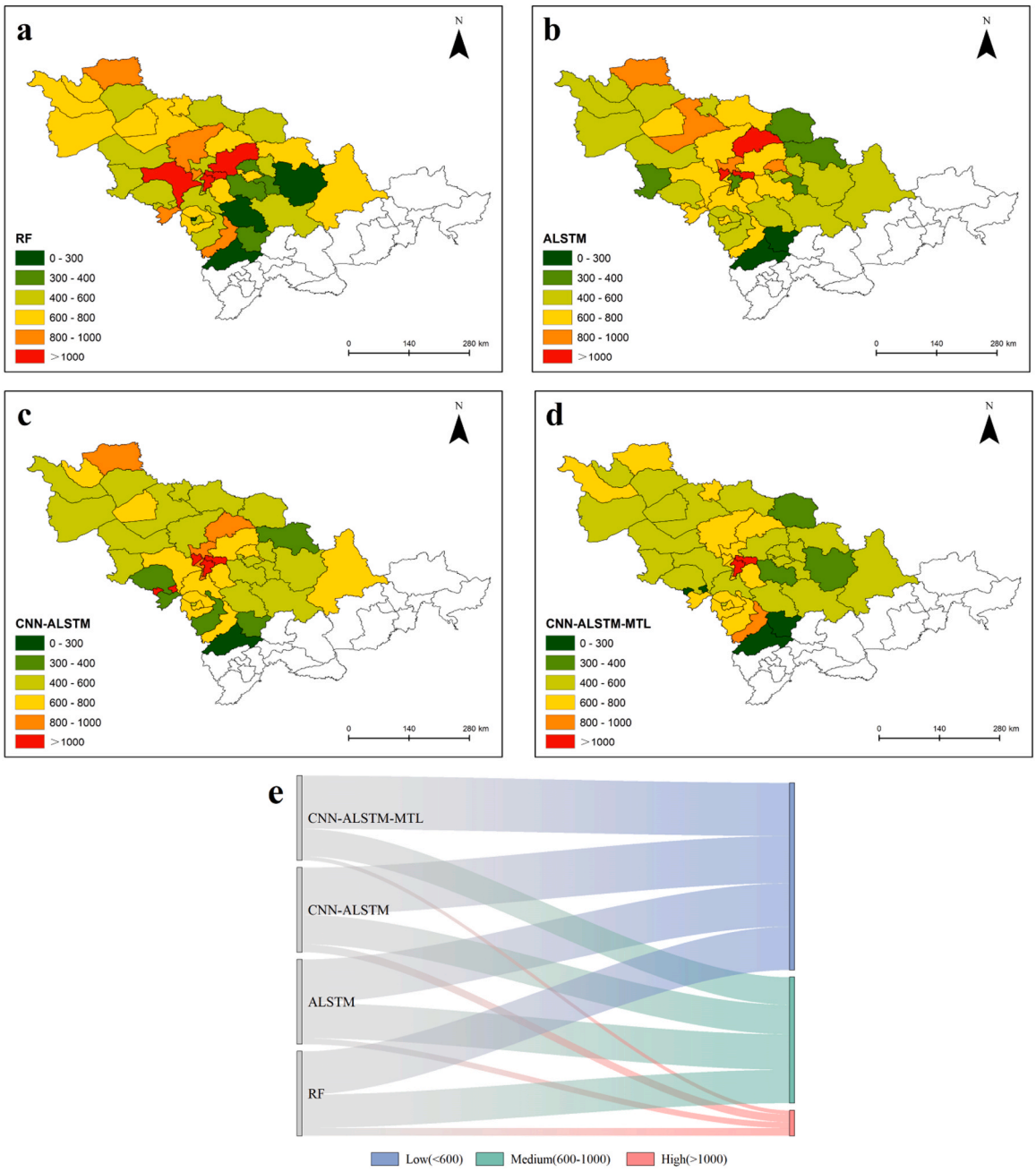


Fig. 15. Spatial distribution and proportion of county-level RMSE for each model under six-fold cross-validation. a, b, and c show the spatial distribution of RMSE for the three models; d shows the distribution of error magnitudes across models.

underscoring the importance of soil variables (Wang et al., 2020a, 2020b). Similarly, Cao et al. compare LSTM and CNN models for county-level wheat yield estimation in China, confirming the superior performance of LSTM and suggesting that combining both models may further enhance prediction accuracy (Cao et al., 2021; Sun et al., 2019). Methods 7–8 establish traditional hybrid frameworks that combine crop growth models with machine-learning techniques to enhance yield prediction capability; however, neither incorporates data assimilation within the crop growth modeling process (Feng et al., 2019, 2020), nor do they consider the influence of spatial heterogeneity on prediction accuracy. Therefore, opportunities remain to achieve earlier and more robust county-level yield prediction while maintaining mechanistic consistency.

To address the aforementioned limitations, a framework that integrates the CNN-ALSTM-MTL model with the ENKF-WOFOST model is proposed on the basis of model structures developed in previous studies. The results indicate that this integrated framework improves prediction accuracy by 35 % in R^2 and reduces RMSE by 23 % compared with the traditional process-based crop growth model. This performance enhancement mainly arises from four key techniques: First, a dynamic time warping (DTW) algorithm is introduced to evaluate the similarity between historical meteorological sequences and the climatic pattern of the target growing season. Representative historical years are selected and concatenated with real-time meteorological observations of the prediction year to generate a complete meteorological sequence for driving the WOFOST model, effectively resolving the challenge of missing future meteorological data; Second, driven by the DTW-reconstructed meteorological data, ENKF assimilation is implemented to progressively update the model state, increasing R^2 by 0.2 and reducing RMSE by 276 kg/ha, thereby providing a stable physical

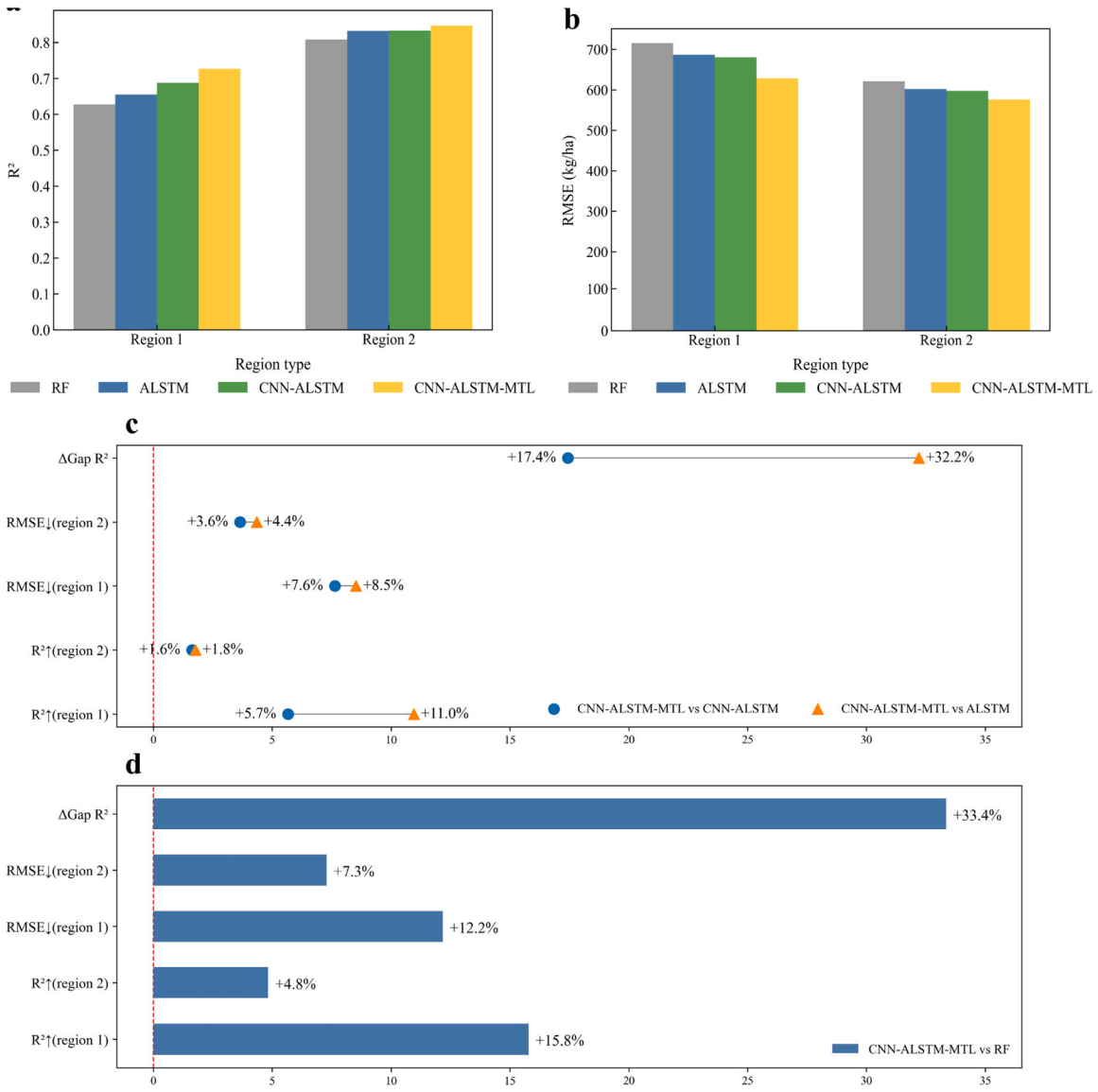


Fig. 16. Prediction performance of each model across different regions and the cross-regional improvements relative to baseline models. a shows the R^2 values of predicted yield versus county-level yield across regions; b presents the RMSE values of predicted yield versus county-level yield across regions; c illustrates the relative improvement of CNN-ALSTM-MTL over ALSTM and CNN-ALSTM; d illustrates the relative improvement of CNN-ALSTM-MTL over the RF model.

Table 2
Comparison of results from different yield prediction methods.

No.	Method	Model	Crop	R^2	RMSE (kg/ha)	Earliest Predictable Stage	Study Area	Source
1	Hybrid Framework	CNN-ALSTM-MTL	Maize	0.75	592	Tasseling Stage	China	This study
2	Machine Learning	XGBoost	Soybean	0.82	/	Blister Stage	United States	Li et al., 2023b
3	Deep Learning	LSTM	Maize	0.67	/	Milk Stage	China	Ji et al., (2022)
4	Deep Learning	LSTM	Wheat	0.75	732	Filling Stage	China	Wang et al., (2020a, 2020b)
5	Deep Learning	CNN	Wheat	0.86	644	Maturity Stage	China	Cao et al., 2021
6	Deep Learning	CNN-LSTM	Soybean	0.73	329	Blister Stage	United States	Sun et al., (2019)
7	Hybrid Framework	RF	Wheat	0.81	540	Filling Stage	Australia	Feng et al., (2019)
8	Hybrid Framework	RF	Wheat	/	700	Filling Stage	Australia	Feng et al., (2020)

baseline for subsequent modeling; Third, a comprehensive deep-learning architecture is constructed to integrate multisource heterogeneous data, including remote-sensing indices, meteorological variables, crop physiological characteristics, soil parameters, and geographic environmental factors. This multisource data-fusion strategy enables the model to better capture the complex nonlinear relationships between maize growth and environmental drivers (Wang et al., 2013; Meng et al., 2019; Liu et al., 2024; Li et al., 2022; Wang et al., 2020a, 2020b); and Fourth, the hybrid CNN-ALSTM-MTL model strengthens spatiotemporal feature extraction and employs multi-task learning (MTL) to share common representations across regions while retaining region-specific outputs, thereby enhancing model stability and generalization capability (Vandenhende et al., 2021; Song et al., 2025). Compared with single-task models, which rely on a single mapping that tends to average

out regional differences and introduce systematic biases in certain areas, the regionalized output structure enables differential optimization for each region on top of shared features. As a result, the overall accuracy is substantially improved (R^2 increases by approximately 4.2 %–13.6 %, and RMSE decreases by 5.1 %–10.4 %), and cross-regional consistency is markedly enhanced (ΔGap R^2 decreases by 17.4 %–33.4 %). This spatiotemporal-fusion and multi-task-collaborative design allows the model to more effectively capture interregional heterogeneity in complex agricultural environments, thereby achieving superior yield-prediction performance.

The predictive skill of the hybrid framework exhibits a progressive improvement as maize development advances. Experimental results show that from T1 to T3, the coefficient of determination (R^2) increases by roughly 40 %, while RMSE decreases by about 26 %, indicating that the model increasingly captures temporal growth dynamics as information accumulates throughout the season. The T3 stage (jointing to tasseling stage) is particularly critical, as it corresponds to peak canopy photosynthetic efficiency and rapid biomass accumulation. Physiologically, T3 marks a period of accelerated canopy expansion and maximum light-use efficiency, during which dry matter accumulates rapidly and the foundation for subsequent grain-number formation is established. Consequently, environmental signals during this stage exhibit the strongest linkage with final yield. In contrast, information newly added at T4 primarily reflects grain filling and kernel-weight determination and overlaps substantially with signals already captured in earlier stages, resulting in limited marginal improvement to overall model performance. From a data perspective, on the one hand, the LAI inversion in this study shows higher consistency with the reference products during T3, whereas systematic deviations are more likely to occur in T4, indicating that canopy-state information is "cleaner" at T3. On the other hand, the DTW-reconstructed meteorological data for the target year show better temporal completeness and consistency during T3–T4, thereby reducing driving noise and stabilizing state updating. The combined effects of these two factors jointly enhance the effective signal-to-noise ratio at T3, enabling the model to achieve superior predictive performance during this key yield-formation window and to deliver earlier and more reliable decision support. These results further validate the potential of the hybrid framework for dynamic growth-stage monitoring and time-sensitive crop management.

Overall, the proposed hybrid framework—integrating DTW-based weather selection, crop model assimilation outputs, and deep learning techniques—outperforms single models and conventional fusion approaches in terms of predictive accuracy, model robustness, and regional adaptability. In county-level maize yield prediction across Jilin Province, the framework achieves an overall RMSE of 592 kg/ha and maintains low error variability across regions, indicating strong spatial generalization capacity. These results not only confirm the effectiveness of the target-year weather substitution strategy but also underscore the strong potential of deep learning for integrating multi-source data and mining crop growth potential.

4.2. Limitations and future directions

The hybrid framework proposed in this study demonstrates strong performance in county-level maize yield prediction and verifies its applicability under regional heterogeneity. Nevertheless, several limitations remain and warrant further refinement in future research.

With respect to data quality, the overall performance of the proposed framework is primarily constrained by two factors. First, the model exhibits strong dependence on the completeness of input data and on the quality of crop-model outputs after data assimilation, including the availability and preprocessing of remote-sensing and meteorological inputs, as well as the specification of observation errors in the ENKF. Under conditions where remote-sensing observations are sparse, of limited quality, or lack broad-coverage local error statistics, uncertainties in input and observation-error specification can be propagated through assimilation into state estimates, thereby affecting the subsequent deep-learning module and reducing overall predictive accuracy. Second, the meteorological sequences constructed using DTW rely heavily on the quality and temporal continuity of the historical meteorological candidate set. When historical records contain episodic data gaps or systematic biases, matching uncertainties can easily arise. In addition, under extreme climatic conditions, the stage-wise progression of the target year may deviate from historical patterns, which can also introduce matching uncertainty and thereby lead the ENKF–WOFOST outputs to diverge from actual crop development, ultimately affecting predictive accuracy. To mitigate this risk, extreme-climate indicators such as KDD, FDD, and EPA are introduced into the hybrid framework to adaptively modulate the dependence on ENKF–WOFOST outputs and to implement residual corrections, thereby enhancing the model's capability to represent anomalous conditions. The reliability of the framework has been verified for typical years, and future work will further assess its applicability under extreme-climate years.

Regarding uncertainties arising from meteorological reconstruction, future work will integrate ensemble forecasting and climate scenarios to generate multiple candidate meteorological drivers and thereby develop a probabilistic yield-prediction system to quantify reconstruction uncertainty, reduce dependence on a single DTW-reconstructed sequence, and mitigate bias propagation when mismatches occur. Meanwhile, permutation-based importance analyses will be conducted by growth stage from T1 to T4 to quantify the contributions of KDD, FDD, and EPA at different stages, and these results will be reported concurrently with the interval-based prediction outcomes.

With respect to within-season dynamic forecasting, yield predictions are conducted stage-by-stage based on a division of the crop growth cycle into four phases (T1 to T4). However, these divisions are based on fixed temporal windows and fail to account for interannual phenological shifts induced by climate variability (e.g., delayed sowing, early tasseling). This may lead to misalignment between predefined stages and the actual physiological status of the crop, thereby posing challenges in assessing the impacts of extreme weather events. While general indicators of climatic extremes—such as accumulated heat stress, cold stress, and heavy precipitation—are already included in the model, stage-specific indicators tailored to the key physiological processes of each growth phase have not yet been established. Future research should dynamically construct phenology-specific extreme weather indices based on the physiological requirements and sensitivity of crops at each developmental stage, rather than relying on uniform climate indicators, to enhance the model's responsiveness to yield variability in abnormal years.

With respect to cross-crop and cross-regional applications, the current framework is designed for county-level spring maize in Jilin Province. Its applicability to double-cropping systems (e.g., winter-wheat–maize rotations) has not yet been evaluated. Extending the framework to such systems requires crop- and season-specific segmentation as well as the construction of separate county-level yield labels for different crops (or seasons), accompanied by corresponding adjustments to data assimilation and model configurations. Therefore, generalizing the framework from spring maize in Jilin Province to other crops or other regions is not a direct "transfer." The associated risks fall into two categories. The first concerns cross-crop transfer: (1) the cultivar parameters of the WOFOST model must be recalibrated for each crop; (2) the DTW-based meteorological sequences need to be aligned according to phenological stages—for example, winter wheat requires cross-year alignment to account for "overwintering–regreening"; and (3) the feature weights in the deep-learning module must be re-estimated. The second involves cross-regional transfer: (1) the thermal-resource zoning of the target region must be redefined, and the corresponding output heads in the MTL structure must be reset; and (2) spatial aggregation schemes and evaluation metrics must be standardized to ensure consistency between label and feature scales, preventing aggregation-

induced biases. Accordingly, future applications will follow a standardized pipeline: recalibration of crop-model parameters → phenology-aligned DTW reconstruction → ENKF–WOFOST assimilation and prediction → regional reclassification and output-head resetting → model retraining or fine-tuning. Performance improvements in R^2 and RMSE, together with advances in the earliest available prediction window, will serve as the primary criteria for evaluating reproducibility and robustness in cross-crop and cross-regional transfer.

With respect to spatial scale, the application scenario of this study is confined to county-level maize yield prediction. This design is advantageous for supporting county-scale yield monitoring and decision-making, but it inevitably smooths fine-scale, within-county field heterogeneity. As a result, the current framework is not able to directly characterize yield fluctuations at the level of individual fields or experimental plots. Accordingly, all conclusions are restricted to the county scale and are not intended to be extrapolated directly to the field scale. If, in the future, a sufficient number of plot-level yield observations that are strictly co-registered with satellite overpasses become available, field-scale applications could be explored in an exploratory manner—for example, by conducting tentative validation analyses at the field scale and, where appropriate, investigating potential extensions of the framework—to assess the feasibility and limitations of applying the proposed approach at finer spatial resolutions.

Overall, future research can be expanded in several directions. First, high-spatiotemporal-resolution remote-sensing and meteorological data may be incorporated to improve the statistical characterization of observation errors, and alternative data-assimilation schemes may be compared on the basis of the current ENKF configuration to more comprehensively describe error structures and anomalous processes, thereby enhancing the model's responsiveness to early warning signals and short-term anomalies. With respect to assimilation settings, if spatially explicit fertilizer-application data become available, nitrogen-limitation scenarios could be introduced for sensitivity analyses to quantify the impacts and uncertainties associated with nitrogen-related parameter settings, thereby improving the credibility of yield estimates. Second, multi-scenario climate simulations may be integrated to generate yield predictions under different climate-change pathways, improving adaptability during anomalous years. Third, stage-specific response systems to extreme climatic conditions may be developed to enable dynamic updates and matching of stage-wise climate indicators, thereby strengthening stage-dependent sensitivity and early-season usability. Fourth, a standardized implementation pathway for cross-crop and cross-regional extensions may be established to ensure broader applicability across more crop types and geographical regions. Fifth, under richer data conditions and unified data formats, a broader set of mainstream deep-learning models may be evaluated to further examine the adaptability and robustness of the proposed framework.

5. Conclusion

This study proposes and validates a hybrid framework (ENKF-WOFOST + CNN-ALSTM-MTL) that integrates remote-sensing data assimilation, process-based crop modeling, and deep learning to improve the accuracy and timeliness of county-level maize yield prediction under regional heterogeneity. Meteorological sequences for the target year are generated using a dynamic time warping (DTW) algorithm and are subsequently employed to drive the assimilated WOFOST model for yield estimation across different growth stages. The assimilated outputs are then combined with multisource heterogeneous data to train a CNN-ALSTM-MTL model, enhancing the characterization and use of spatiotemporal features during crop development. The results indicate that assimilation substantially strengthens the model's capacity to capture both crop growth processes and yield, and that, under the DTW-constructed meteorological sequence, it produces reliable estimates of target-year yield. Integrating the assimilated crop model with deep learning further improves predictive performance, which increases steadily as the growing season progresses, enabling forward-looking decision support at key growth stages. In the future, on the basis of standardized implementation across crops and regions and with continued advances in remote-sensing observation, meteorological forecasting, and artificial intelligence, the hybrid framework is expected to be applied at larger spatial scales and to a broader range of crop types, strengthening China's food security and agricultural risk management.

CRediT authorship contribution statement

Jun Gao: Writing – original draft, Visualization, Software, Methodology, Conceptualization. **Daming Dong:** Writing – review & editing, Supervision, Methodology, Conceptualization. **Wenjiang Huang:** Writing – review & editing. **Yingying Dong:** Writing – review & editing. **Tongren Xu:** Writing – review & editing, Resources. **Chongya Jiang:** Resources, Data curation. **Kun Wang:** Writing – review & editing, Supervision, Project administration, Methodology, Conceptualization.

Declaration of Competing Interest

The authors declare that they have no known competing financial interests or personal relationships that could have appeared to influence the work reported in this paper.

Acknowledgements

This work was supported by the Science and Technology Project of the Ministry of Agriculture and Rural Affairs of China and the National Natural Science Foundation of China (Grant No. 32271986).

Appendix A. Supporting information

Supplementary data associated with this article can be found in the online version at doi:10.1016/j.eja.2025.127977.

Data availability

The authors do not have permission to share data.

References

Alam, M.M.T., Simic Milas, A., Gašparović, M., Osei, H.P., 2024. Retrieval of crop canopy chlorophyll: machine learning vs. radiative transfer model. Remote Sens. 16 (12), 2058.

Alimagham, S., van Loon, M.P., Ramirez-Villegas, J., Berghuijs, H.N., Rosenstock, T.S., van Ittersum, M.K., 2025. Integrating crop models and machine learning for projecting climate change impacts on crops in data-limited environments. Agric. Syst. 228, 104367.

Ansarifar, J., Wang, L., Archontoulis, S.V., 2021. An interaction regression model for crop yield prediction. Sci. Rep. 11 (1), 17754.

Bai, H., Xiao, D., Tang, J., Liu, D.L., 2024. Evaluation of wheat yield in North China Plain under extreme climate by coupling crop model with machine learning. Comput. Electron. Agric. 217, 108651.

Basso, B., Liu, L., 2019. Seasonal crop yield forecast: Methods, applications, and accuracies. Adv. Agron. 154, 201–255.

Benkendorf, D.J., Hawkins, C.P., 2020. Effects of sample size and network depth on a deep learning approach to species distribution modeling. Ecol. Inform. 60, 101137.

Brown, J.N., Hochman, Z., Holzworth, D., Horan, H., 2018. Seasonal climate forecasts provide more definitive and accurate crop yield predictions. Agric. For. Meteorol. 260, 247–254.

Cai, J., Chen, J., Dou, X., Xing, Q., 2022. Using machine learning algorithms with in situ hyperspectral reflectance data to assess comprehensive water quality of urban rivers. IEEE Trans. Geosci. Remote Sens. 60, 1–13.

Cao, J., Zhang, Z., Luo, Y., Zhang, L., Zhang, J., Li, Z., Tao, F., 2021. Wheat yield predictions at a county and field scale with deep learning, machine learning, and google earth engine. Eur. J. Agron. 123, 126204.

Ceglar, A., Van der Wijngaart, R., De Wit, A., Lecerf, R., Boogaard, H., Seguini, L., Baruth, B., 2019. Improving WOFOST model to simulate winter wheat phenology in Europe: evaluation and effects on yield. Agric. Syst. 168, 168–180.

Chen, Q., Zheng, B., Chen, T., Chapman, S.C., 2022. Integrating a crop growth model and radiative transfer model to improve estimation of crop traits based on deep learning. J. Exp. Bot. 73 (19), 6558–6574.

Chen, S., Jiang, T., Ma, H., He, C., Xu, F., Malone, R.W., He, J., 2020. Dynamic within-season irrigation scheduling for maize production in Northwest China: a method based on weather data fusion and yield prediction by DSSAT. Agric. For. Meteorol. 285, 107928.
Chen, Y., Tao, F., 2022. Potential of remote sensing data-crop model assimilation and seasonal weather forecasts for early-season crop yield forecasting over a large area. Field Crops Res. 276, 108398.
Conradt, T., 2022. Choosing multiple linear regressions for weather-based crop yield prediction with ABSOLUT v1. 2 applied to the districts of Germany. Int. J. Biometeorol. 66 (11), 2287–2300.
De Wit, A., Boogaard, H., Fumagalli, D., Janssen, S., Knapen, R., van Kraalingen, D., van Diepen, K., 2019. 25 years of the WOFOST cropping systems model. Agric. Syst. 168, 154–167.
De Wit, A.D., Van Diepen, C.A., 2007. Crop model data assimilation with the Ensemble Kalman filter for improving regional crop yield forecasts. Agric. For. Meteorol. 146 (1-2), 38–56.
Dong, R., Leng, H., Zhao, J., Song, J., Liang, S., 2022. A framework for four-dimensional variational data assimilation based on machine learning. Entropy 24 (2), 264.
Falcon, W.P., Naylor, R.L., Shankar, N.D., 2022. Rethinking global food demand for 2050. Popul. Dev. Rev. 48 (4), 921–957.
Feng, P., Wang, B., Li Liu, D., Waters, C., Yu, Q., 2019. Incorporating machine learning with biophysical model can improve the evaluation of climate extremes impacts on wheat yield in south-eastern Australia. Agric. For. Meteorol. 275, 100–113.
Feng, P., Wang, B., Liu, D.L., Waters, C., Xiao, D., Shi, L., Yu, Q., 2020. Dynamic wheat yield forecasts are improved by a hybrid approach using a biophysical model and machine learning technique. Agric. For. Meteorol. 285, 107922.
Féret, J.B., Gitelson, A.A., Noble, S.D., Jacquemoud, S., 2017. PROSPECT-D: towards modeling leaf optical properties through a complete lifecycle. Remote Sens. Environ. 193, 204–215.
Hu, T., Zhang, X., Khanal, S., Wilson, R., Leng, G., Toman, E.M., Zhao, K., 2024. Climate change impacts on crop yields: a review of empirical findings, statistical crop models, and machine learning methods. Environ. Model. Softw. 179, 106119.
Huang, J., Sedano, F., Huang, Y., Ma, H., Li, X., Liang, S., Wu, W., 2016. Assimilating a synthetic Kalman filter leaf area index series into the WOFOST model to improve regional winter wheat yield estimation. Agric. For. Meteorol. 216, 188–202.
Ines, A.V., Das, N.N., Hansen, J.W., Njoku, E.G., 2013. Assimilation of remotely sensed soil moisture and vegetation with a crop simulation model for maize yield prediction. Remote Sens. Environ. 138, 149–164.
Jay, S., Maupas, F., Bendoula, R., Gorretta, N., 2017. Retrieving LAI, chlorophyll and nitrogen contents in sugar beet crops from multi-angular optical remote sensing: comparison of vegetation indices and PROSAIL inversion for field phenotyping. Field Crops Res. 210, 33–46.
Jeong, S., Ko, J., Shin, T., Yeom, J.M., 2022. Incorporation of machine learning and deep neural network approaches into a remote sensing-integrated crop model for the simulation of rice growth. Sci. Rep. 12 (1), 9030.
Ji, Z., Pan, Y., Zhu, X., Zhang, D., Dai, J., 2022. Prediction of corn yield in the USA corn belt using satellite data and machine learning: from an evapotranspiration perspective. Agriculture 12 (8), 1263.
Jiang, Z., Chen, Z., Chen, J., Ren, J., Li, Z., Sun, L., 2014. The estimation of regional crop yield using ensemble-based four-dimensional variational data assimilation. Remote Sens. 6 (4), 2664–2681.
Jiao, Q., Sun, Q., Zhang, B., Huang, W., Ye, H., Zhang, Z., Qian, B., 2021. A random forest algorithm for retrieving canopy chlorophyll content of wheat and soybean trained with PROSAIL simulations using adjusted average leaf angle. Remote Sens. 14 (1), 98.
Li, J., Li, G., Wang, L., Li, D., Li, H., Gao, C., Wang, E., 2023a. Predicting maize yield in Northeast China by a hybrid approach combining biophysical modelling and machine learning. Field Crops Res. 302, 109102.
Li, Y., Chang, C., Wang, Z., Li, T., Li, J., Zhao, G., 2022. Identification of cultivated land quality grade using fused multi-source data and multi-temporal crop remote sensing information. Remote Sens. 14 (9), 2109.
Li, Y., Zeng, H., Zhang, M., Wu, B., Zhao, Y., Yao, X., Wu, F., 2023b. A county-level soybean yield prediction framework coupled with XGBoost and multidimensional feature engineering. Int. J. Appl. Earth Obs. Geoinf. 118, 103269.
Liu, Q., Wang, C., Jiang, J., Wu, J., Wang, X., Cao, Q., Liu, X., 2024. Multi-source data fusion improved the potential of proximal fluorescence sensors in predicting nitrogen nutrition status across winter wheat growth stages. Comput. Electron. Agric. 219, 108786.
Lobell, D.B., Burke, M.B., 2010. On the use of statistical models to predict crop yield responses to climate change. Agric. For. Meteorol. 150 (11), 1443–1452.
Lu, Y., Li, P., Wang, P., Li, T., Li, G., 2025a. A method of rice yield prediction based on the QRBILSTM-MHSA network and hyperspectral image. Comput. Electron. Agric. 239, 110884.
Lu, Y., Zhou, H., Wang, P., Wang, E., Li, G., Yu, T., 2025b. IMobileTransformer: A fusion-based lightweight model for rice disease identification. Eng. Appl. Artif. Intell. 161, 112271.
Luo, L., Sun, S., Xue, J., Gao, Z., Zhao, J., Yin, Y., Luan, X., 2023. Crop yield estimation based on assimilation of crop models and remote sensing data: a systematic evaluation. Agric. Syst. 210, 103711.
Meng, L., Liu, H., Zhang, X., Ren, C., Ustin, S., Qiu, Z., Guo, D., 2019. Assessment of the effectiveness of spatiotemporal fusion of multi-source satellite images for cotton yield estimation. Comput. Electron. Agric. 162, 44–52.
Moriondo, M., Giannakopoulos, C., Bindi, M., 2011. Climate change impact assessment: the role of climate extremes in crop yield simulation. Clim. Change 104 (3), 679–701.
Pan, H., Chen, Z., de Wit, A., Ren, J., 2019. Joint assimilation of leaf area index and soil moisture from sentinel-1 and sentinel-2 data into the WOFOST model for winter wheat yield estimation. Sensors 19 (14), 3161.
Rivera, J.P., Verrelst, J., Leonenko, G., Moreno, J., 2013. Multiple cost functions and regularization options for improved retrieval of leaf chlorophyll content and LAI through inversion of the PROSAIL model. Remote Sens. 5 (7), 3280–3304.
Sajid, S.S., Shahhosseini, M., Huber, I., Hu, G., Archontoulis, S.V., 2022. County-scale crop yield prediction by integrating crop simulation with machine learning models. Front. Plant Sci. 13, 1000224.
Semenov, M.A., Porter, J.R., 1995. Climatic variability and the modelling of crop yields. Agric. For. Meteorol. 73 (3-4), 265–283.
Sinha, S.K., Padalia, H., Dasgupta, A., Verrelst, J., Rivera, J.P., 2020. Estimation of leaf area index using PROSAIL based LUT inversion, MLRA-GPR and empirical models: case study of tropical deciduous forest plantation, North India. Int. J. Appl. Earth Obs. Geoinf. 86, 102027.
Song, H., Zhuang, T., Li, X., Ruan, G., Schepers, J., Wang, D., Cao, Q., 2025. Enhancing winter wheat growth indicator prediction with multi-task learning and multi-source data. Eur. J. Agron. 168, 127629.
Stockwell, D.R., Peterson, A.T., 2002. Effects of sample size on accuracy of species distribution models. Ecol. Model. 148 (1), 1–13.
Sun, J., Di, L., Sun, Z., Shen, Y., Lai, Z., 2019. County-level soybean yield prediction using deep CNN-LSTM model. Sensors 19 (20), 4363.
Sun, J., Wang, L., Shi, S., Li, Z., Yang, J., Gong, W., Tagesson, T., 2022. Leaf pigment retrieval using the PROSAIL model: Influence of uncertainty in prior canopy-structure information. Crop J. 10 (5), 1251–1263.
Van Diepen, C.V., Wolf, J.V., Van Keulen, H., Rappoldt, C., 1989. WOFOST: a simulation model of crop production. Soil Use Manag. 5 (1), 16–24.
Vandenhende, S., Georgoulis, S., Van Gansbeke, W., Proesmans, M., Dai, D., Van Gool, L., 2021. Multi-task learning for dense prediction tasks: a survey. IEEE Trans. Pattern Anal. Mach. Intell. 44 (7), 3614–3633.
Wang, J., Li, X., Lu, L., Fang, F., 2013. Estimating near future regional corn yields by integrating multi-source observations into a crop growth model. Eur. J. Agron. 49, 126–140.
Wang, K., Ma, C., Qiao, Y., Lu, X., Hao, W., Dong, S., 2021. A hybrid deep learning model with 1DCNN-LSTM-Attention networks for short-term traffic flow prediction. Phys. A Stat. Mech. Appl. 583, 126293.
Wang, X., Huang, J., Feng, Q., Yin, D., 2020a. Winter wheat yield prediction at county level and uncertainty analysis in main wheat-producing regions of China with deep learning approaches. Remote Sens. 12 (11), 1744.
Wang, Y., Zhang, Z., Feng, L., Du, Q., Runge, T., 2020b. Combining multi-source data and machine learning approaches to predict winter wheat yield in the conterminous United States. Remote Sens. 12 (8), 1232.
Wanthanaporn, U., Supit, I., Chaowiwat, W., Hutjes, R.W., 2024. Skill of rice yields forecasting over Mainland Southeast Asia using the ECMWF SEAS5 ensemble prediction system and the WOFOST crop model. Agric. For. Meteorol. 351, 110001.
Wu, S., Yang, P., Chen, Z., Ren, J., Li, H., Sun, L., 2021. Estimating winter wheat yield by assimilation of remote sensing data with a four-dimensional variation algorithm considering anisotropic background error and time window. Agric. For. Meteorol. 301, 108345.
Zare, H., Weber, T.K., Ingwersen, J., Nowak, W., Gayler, S., Streck, T., 2024. Within-season crop yield prediction by a multi-model ensemble with integrated data assimilation. Field Crops Res. 308, 109293.
Zhuang, H., Zhang, Z., Cheng, F., Han, J., Luo, Y., Zhang, L., Tao, F., 2024. Integrating data assimilation, crop model, and machine learning for winter wheat yield forecasting in the North China Plain. Agric. For. Meteorol. 347, 109909.